January 2016

A role for the classical complement pathway in hippocampal dendritic injury and hippocampal dependent memory deficits in a model of acquired epilepsy

Nicole Denise Schartz
Purdue University

Graduate School Form 30
Updated 1/15/2015

PURDUE UNIVERSITY
GRADUATE SCHOOL
Thesis/Dissertation Acceptance

This is to certify that the thesis/dissertation prepared

By Nicole Denise Schartz

Entitled

A Role for the Classical Complement Pathway in Hippocampal Dendritic Injury and Hippocampal Dependent Memory Deficits in a Model of Acquired Epilepsy

For the degree of Master of Science

Is approved by the final examining committee:

Amy L. Brewster
Chair

Kimberly P. Kinzig

Susan Sangha

Christie L. Sahley

To the best of my knowledge and as understood by the student in the Thesis/Dissertation Agreement, Publication Delay, and Certification Disclaimer (Graduate School Form 32), this thesis/dissertation adheres to the provisions of Purdue University's "Policy of Integrity in Research" and the use of copyright material.

Approved by Major Professor(s): Amy L. Brewster

Approved by: Janice R. Kelly 7/22/2016

Head of the Departmental Graduate Program Date

A ROLE FOR THE CLASSICAL COMPLEMENT PATHWAY IN HIPPOCAMPAL DENDRITIC INJURY AND HIPPOCAMPAL DEPENDENT MEMORY DEFICITS IN A MODEL OF ACQUIRED EPILEPSY

A Thesis

Submitted to the Faculty

of

Purdue University

by

Nicole Denise Schartz

In Partial Fulfillment of the

Requirements for the Degree

of

Master of Science

August 2016

Purdue University

West Lafayette, Indiana

TABLE OF CONTENTS

Page

LIST OF FIGURES

Figure Page

Figure Page

Figure Page

Figure Page

ABSTRACT

Schartz, Nicole Denise. M.S., Purdue University, August 2016. A Role for the Classical Complement Pathway in Hippocampal Dendritic Injury and Hippocampal Dependent Memory Deficits in a Model of Acquired Epilepsy. Major Professor: Amy L. Brewster.

Status epilepticus (SE) triggers pathological changes to hippocampal dendrites that may promote epileptogenesis. The microtubule associated protein 2 (Map2) helps stabilize microtubules of the dendritic cytoskeleton. Recently, we reported a substantial decline in Map2 that coincided with robust microglia accumulation in the CA1 hippocampal region after an episode of SE. A spatial correlation between Map2 loss and reactive microglia was also reported in human cortex from refractory epilepsy. New evidence supports that microglia are guided by proteins of the classical complement pathway (C1q and C3) to prune dendritic structures. Furthermore, components of complement have been shown to be upregulated in human and experimental epilepsy. Thus, to identify a potential role of the classical complement pathway in SE-induced Map2 and microglial changes, we characterized the spatiotemporal profile of these events. We used immunohistochemistry to determine the distribution of Map2 and the microglia marker IBA1 in the hippocampus after pilocarpine-induced SE from 4 hours to 35 days. We found a decline in Map2

immunoreactivity in the CA1 area that reached minimal levels at 14 days post-SE and partially increased thereafter. In contrast, maximal microglia accumulation occurred in the CA1 area at 14 days post-SE. We then mapped the spatiotemporal profile of C1q using immunohistochemistry at 3-35 days after SE, where substantial Map2 and microglial alterations were observed. We used western blot to determine the levels of C3 and its cleavage products. C1q and C3 were both increased in the hippocampus at 14 days after SE, when Map2 and microglia changes were most profound. Our data indicate that SE-induced Map2 and microglial changes parallel each other's spatiotemporal profiles. These findings also suggest a potential role for the classical complement pathway in SE-induced Map2-microglial interactions.

Cognitive deficits are often associated with epilepsy and experimental models of SE and TLE, particularly because the hippocampus is often vulnerable to injury in TLE. To test the potential role of the classical complement pathway in SE-induced hippocampal injury and hippocampal-dependent cognitive deficits, we used a pharmacological approach to block the classical complement pathway with the C1 esterase inhibitor (C1-Inh). This drug was given at 4-, 24-, and 48-hours after SE. Tissue was collected at 3-, 14-, 25-, and 35-days after SE and a separate cohort of animals were used to test the effects of C1-Inh on cognitive performance using the novel object recognition (NOR) and the Barnes maze (BM) tests. We found that C1-Inh had no effect on hippocampal Map2 loss after SE when compared with hippocampi from the SE groups. Furthermore, microgliosis was exacerbated with C1-Inh

treatment, with a significant increase lasting from 3 days to 35 days after SE. We replicated previous studies showing a deficit in the NOR and BM tests after SE. However, C1-Inh treatment did not attenuate these deficits, and in fact exacerbated the effects in the BM. Taken together, these data support the idea that the classical complement pathway may play a role in epileptogenesis, inflammation, and cognitive deficits, but more experiments are needed to understand what the specific proteins and mechanisms are involved. Future experiments will look at alternative targets within the classical pathway after SE.

INTRODUCTION

Epilepsy: A Clinical Problem

Epilepsy is one of the most common neurological disorders, affecting 65 million people world-wide (Thurman et al., 2011). According to the Epilepsy Foundation, one in 26 people will develop epilepsy in their lifetime, and one third of people with epilepsy do not respond to currently available anti-epileptic drugs (AEDs). Epilepsy is a seizure disorder which consists of spontaneous recurrent seizures (SRS) (Scharfman, 2007). Seizures are characterized by aberrant synchronous neuronal activity consisting of high amplitude and high frequency (200-500 Hz) spikes (Scharfman, 2014). The cause of this increase neuronal activity is thought to be an imbalance of excitatory and inhibitory synapses (Badawy, Harvey, & Macdonell, 2009), but the underlying mechanisms are poorly understood.

Epilepsy is considered a spectrum disorder. There are many different types of epilepsies, varying in number of occurrences, location, severity, and onset of seizures (Jacobs et al., 2009). There are over a dozen types of epilepsy syndromes; some stem from genetics and some are acquired mechanisms. Several single gene mutations have been identified in epilepsy. However, the majority of epilepsy disorders involve far more complex

inheritance, and the development of spontaneous seizures is most likely due to an interaction of several gene mutations and the environment (Berkovic, Mulley, Scheffer, & Petrou, 2006). Genetic disorders associated with seizures include Fragile X Syndrome, Angelman's Syndrome, and generalized epilepsy with febrile seizures plus, among others. Mutations of genes that code for voltage gated potassium, sodium, and chloride channels have been shown to be involved in epilepsies, as they are responsible for altering membrane excitability (Steinlein, 2004). Although it is widely known as a seizure disorder, people with epilepsy have an increased risk of several comorbidities including cognitive impairments, anxiety, and autism, among others (Stafstrom, 2014).

Temporal Lobe Epilepsy

Temporal lobe epilepsy (TLE) is a form of epilepsy that is defined by the occurrence of at least two unprovoked epileptic seizures over a period of at least 24 hours, and can be genetic or acquired (Wiebe, 2000). Medial temporal lobe epilepsy (mTLE) originates in the amygdalo-hippocampal area and is often resolved with surgery, when surgery is an option, because most cases are refractory to pharmaceutical interventions (Téllez-Zenteno & Hernández-Ronquillo, 2012). Individuals with pharmacoresistant (intractable) mTLE report poorer quality of life; including increased depression, social isolation, and unemployment (Alonso-Vanegas et al., 2013). People with intractable mTLE sometimes are not candidates for surgery because, for instance, their seizures originate from more than one area in the brain. When intractable mTLE cannot be resolved with surgery, little or no treatment options remain. TLE can be the

result of genetics, developmental malformation, or brain injury including events such as traumatic brain injury, stroke, and prolonged continuous seizures due to fever and infections among others (acquired epilepsy) (Aird, Venturini, & Spielman, 1967; Neppe, 1981). mTLE is often associated with injury to the hippocampus which results in hippocampal sclerosis and neurodegeneration, and synaptic and network remodeling (Rao, Hattiangady, Reddy, & Shetty, 2006). Some experimental models of mTLE suggest that neurodegeneration may be a contributor to the generation of an epileptic brain, while others suggest that it is a consequence of dendritic and synaptic remodeling within the hippocampal network (Rao et al., 2006). However, the mechanisms that deeply impact hippocampal neuronal and dendritic stability and neuronal hyperexcitability in TLE remain elusive.

Epileptogenesis

As mentioned above, events such as traumatic brain injury, fever, infections, or stroke can precipitate a long-lasting continuous seizure (status epilepticus; SE). SE is diagnosed when the seizures become prolonged and continue for 15 minutes or more, or if there is a period of intermittent seizures without regaining consciousness for the same amount of time (Chapman, Smith, & Hirsch, 2001; Nair, Kalita, & Misra, 2011). Extensive evidence suggest that a single episode of SE is sufficient to turn a normal brain into an epileptic brain (Curia, Longo, Biagini, Jones, & Avoli, 2008), and often mTLE and cognitive comorbidities follow (Brewster et al., 2013; Cavalheiro et al., 1991; Leite, Bortolotto, & Cavalheiro, 1990; Nair et al., 2011). The transition

period from a normal brain to an epileptic brain is known as epileptogenesis. This phenomenon has been observed in humans and in experimental models such as the pilocarpine model of SE and acquired mTLE, in which epileptogenesis occurs during a seizure-free “latent period” that starts after an initial SE episode (Jefferys, 2010).

Neuronal injury associated with an episode of SE and subsequent seizures that further alter neuronal networks can contribute to an even more hyper-excitable circuitry and SRS. SE often precipitates damage to hippocampal neuronal and dendritic elements (do Nascimento et al., 2012; Rao et al., 2006; Swann, Al-Noori, Jiang, & Lee, 2000). During the latent period after SE, there are changes in connectivity, particularly in the CA1 region of the hippocampal formation (Brewster et al., 2013; Jung et al., 2009; Rao et al., 2006; Schartz et al., 2016). Also, studies using electron microscopy have shown that after seizures, axons of the dentate gyrus (DG) in the hippocampus expand and innervate dendrites in novel areas, and this re-organization is unique to epileptic brains (Scharfman, 2007). Furthermore, it has been suggested that neuronal injury due to seizures, accompanied by the release of inflammatory signals (e.g., TNF-alpha, IL-1beta), triggers microglia activation and subsequent inflammation and phagocytosis of these stressed neurons (Andersson, Perry, & Gordon, 1991; Borges et al., 2003; Eyo, Murugan, & Wu, 2016; Eyo et al., 2014; Turrin & Rivest, 2004; Vezzani et al., 1999). Loss of hippocampal neurons may promote formation of excitatory axonal pathways, and this excitement may be exacerbated by a loss of inhibitory pathways

(Dingledine, Varvel, & Dudek, 2014). Evidence suggests a role of microglia in the development of epilepsy. During the latent period, there is an accumulation of microglia in the hippocampus paired with a loss of neuronal and dendritic markers (Rao et al., 2006; Schartz et al., 2016). Pre-treatment as well as treatment up to two weeks after SE with a potent immunosuppressant attenuates neuronal and dendritic alterations associated with SE, as well as cognitive impairments and may attenuate the occurrence of SRS after the latent period (Brewster et al., 2013; Guo et al., 2016; Huang et al., 2010; Wang et al., 2015; Zeng, Rensing, & Wong, 2009). Taken together these studies suggest a role for immune cells and neuroinflammation in the dendritic pathology associated with SE and epilepsy.

Cognitive and Behavioral Deficits in SE and mTLE

Individuals with severe mTLE can have decreased cognitive function (Abrahams et al., 1999; Guerreiro, Jones-Gotman, Andermann, Bastos, & Cendes, 2001), which may contribute to self-reported poor quality of life. In the pilocarpine model of acquired TLE, rats display similar cognitive dysfunction (Brewster et al., 2013; Chauviere et al., 2009; Hort, Brożek, Mareš, Langmeier, & Komárek, 1999; Pearson, Schulz, & Patel, 2014). The hippocampus has been implicated as the area of the brain responsible for integrating information into long term memory, as well as for spatial memory (Schenk & Morris, 1985; Scoville & Milner, 1957). As early as 1 week after SE, there is a decrease in the immunoreactivity (IR) to neuronal marker NeuN and dendritic marker microtubule associated protein-2 (Map2) in the CA1 area of the hippocampus

in animal models (Rao et al., 2006; Schartz et al., 2016). Using behavioral tests that assess hippocampal-dependent memory tasks, such as novel object recognition (NOR) and Morris water maze (MWM), it has been established that the pilocarpine model of SE results in a long-lasting deficit in retention of information, detectable as early as 5 days after SE (Brewster et al., 2013; Pearson et al., 2014). Previous studies using the NOR test in rats that have undergone SE established a deficit of SE rats in distinguishing between familiar and novel objects after a 24 hour retention period. Tests like the MWM also show a deficit in spatial memory in pilocarpine treated rodents, however this test may not be appropriate for this model because of the physical aspects of epilepsy (e.g. unprovoked seizures) (Brewster et al., 2013; Murphy, 2013). In the MWM, rodents are placed in a pool of opaque water and must find a hidden platform guided by visual cues placed around the testing room. This test is effective, but could potentially be dangerous in an epileptic rodent. At the time point of testing, some rats are exhibiting spontaneous seizures, which could be fatal if it occurs during the MWM. An alternative to the MWM is the Barnes maze (BM). This test uses the same rationale and general design as the MWM, but eliminates the water. Instead, rats are placed on a circular platform with one escape hole that the rat has to find using spatial cues placed around the room. Both reward (food) and anxiogenic conditions (bright light or loud noise) can be used to make the rodent enter the escape hole. Previous studies have found deficits in this test in a mouse model of epilepsy (Levin, Serrano, &

Dingledine, 2012). Therefore, the BM test is an appropriate measure of spatial memory in models of SE and acquired epilepsy.

Specific Evidence for Dendritic/Neuronal Damage

Dendrites make up most of a neuron's surface area, where numerous neurotransmitter receptors and ion channels play a critical role in shaping the response to synaptic inputs under physiological conditions and in epilepsy. SE is associated with altered dendritic stability of hippocampal neurons. For instance, dendritic size and number of branches have repeatedly been reported to decrease in epilepsy (Swann et al., 2000; Wong, 2005). Map2 is critical for microtubule assembly and thereby for structural stability of the dendritic cytoskeleton (Dehmelt & Halpain, 2004). Pharmaco-genetic manipulations of Map2 protein have elucidated its roles in intracellular trafficking, dendritic plasticity, stability and spine growth (Harada, Teng, Takei, Oguchi, & Hirokawa, 2002). Seizures result in altered levels and distribution of Map-2 in the hippocampus (Ballough et al., 1995; Dachet et al., 2015; Jalava, Lopez-Picon, Kukko-Lukjanov, & Holopainen, 2007; Schartz et al., 2016). Evidence suggest that seizures are associated with decreases of Map2 IR (Ballough et al., 1995), a clear indicator of brain damage. Dendritic alterations have been found in both clinical cases and animal models of epilepsy (Brewster et al., 2013; Dachet et al., 2015; Ma, Ramachandran, Ford, Parada, & Prince, 2013; Schartz et al., 2016).

In some instances, the loss of Map2 may be directly associated with neuronal loss which can occur in the CA1 hippocampal region originating from

chronic intractable epilepsy. In parallel, immunostaining of such tissue has revealed accumulation of astrocytes and microglia in the epileptic focus (Aronica et al., 2007; Dachet et al., 2015). High magnification immunofluorescence has revealed that after an episode of SE, there is a decrease in dendritic marker Map2, and microglial marker (IBA1) makes more contacts with dendrites in the hippocampus when compared with control (Brewster et al., 2013). Loss of Map2 occurring in parallel with accumulation of microglia has also been observed in tissue resected from the brains of patients with long-standing epilepsy (Dachet et al., 2015).

Role of Microglia

Microglia are the resident immune cells of the central nervous system and modulate neuroinflammatory responses associated with injury and disease (Kettenmann, Hanisch, Noda, & Verkhratsky, 2011). Pathological circumstances trigger microglia to infiltrate, accumulate, and to develop inflammatory and phagocytic phenotypes that include changes in their morphological appearance from highly ramified to hypertrophied/amoeboid, and the production and release of inflammatory cytokines, chemokines, and trophic factors (Kettenmann et al., 2011). The presence of microglia with hypertrophied or amoeboid morphologies expressing a number of inflammatory proteins is a feature often seen in hippocampal tissue resected from individuals with intractable temporal lobe epilepsy and widely observed in association with seizures in experimental animal models (Vezzani, French, Bartfai, & Baram, 2011). Immunohistochemical analyses support activation of microglia in all sub

regions of the hippocampus (e.g. CA1, CA3, and DG) following SE (Amhaoul et al., 2015; Avignone, Ulmann, Levavasseur, Rassendren, & Audinat, 2008; Brewster et al., 2013; M. G. De Simoni et al., 2000; Patterson et al., 2015; Ravizza et al., 2005; Rizzi et al., 2003; Shapiro, Wang, & Ribak, 2008; A. Vezzani & Granata, 2005). Even though little is known about the potential role of microglia in the disruption of dendritic stability after SE, evidence suggest that microglia and its associated neuroinflammatory and phagocytic properties are implicated in neural degeneration along with neuronal structural changes that include aberrant dendritic morphology, altered spine densities, synapse pruning, and axonal sprouting (Allan & Rothwell, 2003; Eyupoglu, Bechmann, & Nitsch, 2003; Horn, Busch, Hawthorne, van Rooijen, & Silver, 2008; Richwine et al., 2008; Shapiro, Korn, & Ribak, 2005; Tremblay et al., 2011; Yang et al., 2010). Taken together, these studies suggest that microglial cells play non-canonical roles in modulating neuronal processes.

Microglia release neuroprotective substances such as brain derived neurotrophic factor (BDNF) and nerve growth factor (NGF), to facilitate neuron repair and regrowth (Mirrione & Tsirka, 2011) and promote anti-inflammatory responses through phagocytosis of apoptotic cells (Tremblay et al., 2011). Additionally, microglia play a role in activity-dependent synaptic remodeling (Schafer, Lehrman, & Stevens, 2013). This has been observed in developmental synaptic pruning in which microglia eliminate extra synapses to allow the remaining synapses to strengthen. Microglia-mediated synaptic pruning has also been observed in pathological conditions (Hong et al., 2016;

Stephan, Barres, & Stevens, 2012). After facial nerve axotomy, activated microglia disconnect the dendrites from axonal terminals (Tremblay et al., 2011). Microglial activation has been reported following seizures in various experimental animal models of epilepsy and in human epileptic tissue (Choi & Koh, 2008; Vezzani & Granata, 2005). Models of SE result in significant activation of microglia in CA1, CA3, and DG areas of the hippocampus (Avignone et al., 2008; Schartz et al., 2016).

Existing evidence suggest that suppression of reactive microglia in models of SE and other neurodegenerative brain injuries is neuroprotective (Brewster et al., 2013; Bye et al., 2007; Guo et al., 2016). Administration of an immunosuppressant after SE inhibits microglia and reduces cognitive and behavioral effects (Brewster et al., 2013). This evidence supports that aberrant microglia activity may play a causal role in damage to neuronal and dendritic components. However, the underlying mechanisms of microglia-mediated injury in epilepsy and after SE remain unclear. Recent evidence indicate that microglia interact with spines and eliminate synapses guided by “find me” and “eat me” signals sent by proteins of the classical complement cascade (Stevens et al., 2007).

Role of the Classical Complement Pathway

The complement system has long been known as first responders of the innate immune system to pathogens or apoptotic cells. Complement activation occurs via the classical, lectin, or alternative pathways. Although each pathway is activated by its own distinct activating molecule, all pathways converge on

the complement protein C3. The classical complement cascade is activated when C1q binds one of its ligands. Once activated, C1q binds to the active proteases C1r and C1s to form the C1 complex. The complex then cleaves the proteins C4 and C2, the cleavage products of which then form the C3 convertase C4b2a, which cleaves to form C3a and C3b, the biologically active peptides. C3b consists of an alpha and beta chain. Cleavage of C3b by factor I produces an inactive form of C3b (iC3b) which remains bound to the target cell/structure. C3 then cleaves into a series of complement components in a sequential manner. These include C3a and C5a which act as chemoattractants to recruit microglia and other immune cells and promote inflammation ("find me"), and C3b and C5b which opsonize, or tag, the cell of interest for phagocytosis ("eat me") (Stephan et al., 2012).

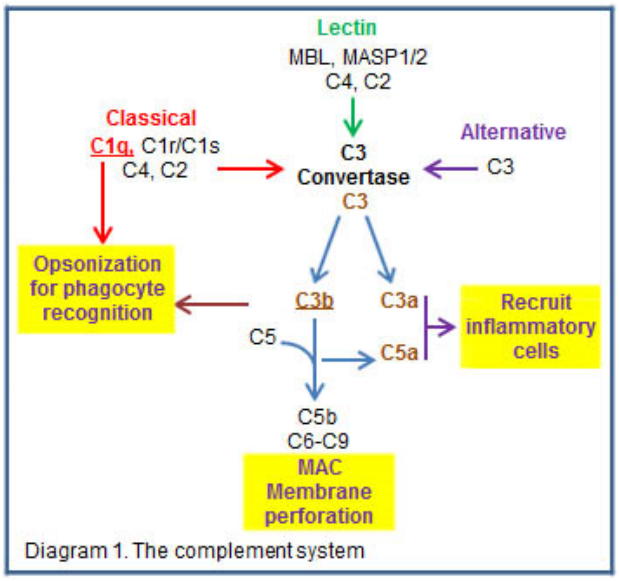

Diagram 1. The complement system

The classical complement cascade has recently been implicated in responses unrelated to inflammation and immune response. Activation of the classical complement cascade during microglia-dependent developmental synaptic pruning (Tremblay et al., 2011) has led to the hypothesis that neurodegeneration is associated with an aberrant reactivation of complement-mediated synaptic pruning as seen in development. Recently, the classical complement pathway has been implicated in neurodegenerative diseases such

as Alzheimer's disease (Hong et al., 2016), multiple sclerosis (Michailidou et al., 2015) and in ischemia (Silverman et al., 2016). Immunohistochemistry and quantitative PCR analysis revealed an increase in a number of classical complement components in surgically removed human TLE tissue, including C1q and C3 , that occurred in the same area where neurodegeneration was observed. In a rat model of TLE, gene expression of complement proteins peaked at one week, corresponding with peak of microgliosis, and was also present at the chronic stages of epilepsy (Aronica et al., 2007). Taken together these data suggest that complement peptides may be a candidate mechanism that guides microglia to eliminate dendrites and in an activity-dependent manner in the epileptic brain.

Hypothesis

Abnormal activation of the classical complement pathway after SE contributes to neuronal and dendritic loss in the CA1 area of the hippocampus, resulting in memory deficits and the development of chronic epilepsy. Inhibition of this pathway may rescue dendrites and neurons and will prevent hippocampal dependent malfunction.

SE promotes activation and proliferation of microglia in the hippocampus. This microgliosis is associated with loss of neuronal and dendritic properties (Brewster et al., 2013; Schartz et al., 2016). High magnification microscopy and three dimensional reconstructions revealed that microglia make physical contacts with dendrites (Kettenmann, Kirchhoff, & Verkhratsky, 2013). After SE, the amount of contacts increases in the CA1

area of the hippocampus (Hasegawa, Yamaguchi, Nagao, Mishina, & Mori, 2007), indicating a possible role of microglia in hippocampal-dendritic pruning and synaptic reorganization in epilepsy. Components of the classical complement pathway have been reported to guide microglia driven dendritic pruning in an activity dependent manner (Schafer et al., 2012). Specific peptides of this pathway such as C3a promote inflammation; and others such as C1q and C3b tag (opsonize) target cells for phagocytosis by microglia (Sarma & Ward, 2011). The findings that microgliosis occurs after SE and that complement proteins guide microglia-mediated phagocytosis led to the question of whether complement expression is altered in SE. In fact, mRNA expression for the classical complement cascade is increased in hippocampal tissue from human and experimental TLE (Aronica et al., 2007). For this reason, we explored the change in protein levels using western blot and spatiotemporal alterations after SE in these complement proteins using immunohistochemistry. To test the hypothesis that the classical complement cascade mediates microgliosis and the resulting injury to neurons and dendrites and the associated cognitive impairments, the pathway will be inhibited by the C1 esterase inhibitor (C1-Inh), which dissociates C1s and C1r from the C1 complex.

Rationale

Deficits in cognitive performance often occur in association with SRS in humans and in rodent models of SE and TLE (Chauviere et al., 2009; Holmes, 2004; Jacobs et al., 2009; Nolan et al., 2003; Swann & Hablitz, 2000; Wong,

2005). These are often accompanied by hippocampal injury, specifically, dendritic injury, spine loss, and neuroinflammation (Brewster et al., 2013; Swann et al., 2000; Vezzani et al., 2011; Wong, 2005). Given that altered complement transcripts are seen in human TLE (Aronica et al., 2007), linked to seizure generation after acute viral infection (Libbey, Kirkman, Wilcox, White, & Fujinami, 2010), associated with cognitive disturbances in Alzheimer's disease (Kolev, Ruseva, Harris, Morgan, & Donev, 2009), and C1q is increased after SE in hippocampus, we hypothesized that if SE-induced increased complement signaling promotes hippocampal-dependent learning and memory deficits then pharmacological complement inhibition will attenuate this pathophysiology. To test this hypothesis, we used a series of behavioral/cognitive tasks in groups of SE animals treated with vehicle or C1-Inh (SE and SE+C1-Inh) compared to sham-treated controls. The extent of microgliosis, along with neuronal and dendritic alterations after SE and the effects of treatment with C1 esterase inhibitor were assessed using IHC and WB. We determined the efficacy of C1-Inh in the hippocampal neuronal and functional pathology using a series of histological, biochemical and behavioral tests (hippocampal-dependent memory function was evaluated using the novel object recognition task and the Barnes maze).

Aim 1: To determine if SE evokes changes in the classical complement cascade and its association with dendritic changes in the hippocampus.

a. Identify the spatiotemporal profile of dendritic and microglia changes after SE. Immunohistochemistry (IHC) was used with antibodies against Map2 and IBA1. IR was quantified using densitometry analysis of different subregions of the hippocampi. Golgi staining was used to further determine alterations in dendritic spine density after SE.
b. Identify how SE alters the levels and distribution of components of the classical complement pathway in the hippocampus. IHC was used to determine distribution and levels of C1q in hippocampal subregions at different time points after SE. Because C3b antibodies specific for histology were not commercially available, western blot (WB) analysis was used to measure protein levels of C3bα, C3bβ, and iC3b using a total C3 antibody specific for western blotting.
c. Identify the cellular and sub-cellular localization of components of the classical complement pathway. Immunofluorescence (IF) was used to determine the colocalization of C1q with Map2.

AIM 2: To test the hypothesis that abnormal classical complement pathway activation after SE contributes to dendritic loss as well as memory and learning deficits during the latent period.

a. Determine the role of the classical complement pathway in SE-induced pathology. Acute treatment with C1-Inh was administered subcutaneously at 4-, 24-, and 48-hours after an episode of SE. Tissue was collected at various time points after SE (3-35 days) and IHC was used to determine distribution and IR levels of Map2 and IBA1 in the hippocampus.
b. Determine the role of the classical complement pathway in SE-induced cognitive deficits. NOR and BM were done at 2 weeks after SE and C1-Inh treatment. Performance in cognitive tasks was compared between control, SE, and SE+C1-Inh groups.

MATERIALS AND METHODS

Animals

Male Sprague Dawley rats (150-250 grams) (Harlan Laboratories) were housed at the Purdue Psychological Sciences Building. Ambient temperature was constantly 22°C, with diurnal cycles of a 12-hour (hr) light and 12-hr dark (8:00 to 20:00 hr). All animals had access to unlimited food and water.

Pilocarpine-Induced Status Epilepticus

Protocol for induction of SE modified from (Brewster et al., 2013). SE was induced in male Sprague Dawley rats using the chemoconvulsant pilocarpine. Thirty minutes before the intraperitoneal (i.p.) administration of pilocarpine hydrochloride (280-300mg/kg; Sigma Chemical Co., St Louis, MO, USA) rats were given scopolamine methyl bromide (1mg/kg, i.p; Sigma Chemical Co., St Louis, MO, USA) to minimize potential peripheral cholinergic effects of the pilocarpine. Control rats were given scopolamine and saline (sham). Behavioral observation was used to monitor seizure activity and recorded on the Racine scale (Racine, 1972). Rats were deemed to be in SE when they reached stage 5 (rearing and falling). After SE had continued for at least 45 minutes, rats were given an i.p. injection of Diazepam (10mg/kg; Hospira Inc., Lake Forest, IL, USA). Rats that were injected with pilocarpine but

did not develop SE were given Diazepam 1-2 hours after the injection of pilocarpine and included in a pilocarpine control group. Two to four hours after Diazepam administration, rats were given 1.5 mL of sterile 0.9% saline i.p. (AddiPak) and were checked daily to ensure proper weight gain and hydration. During the three days of recovery after SE, rats were fed apples, apple sauce, ensure, or fruit loops as needed. I.P. injections of saline were administered as needed as well.

C1 Esterase Inhibitor Treatment

Rats were given Complement C1-esterase inhibitor, human (C1-inh) (EMD Medicals Inc., San Diego, CA, USA) after SE to inhibit the classical complement pathway. C1-Inh targets serine proteases C1r and S1s, thus preventing the formation of C3 convertase via the classical complement pathway. Control and SE rats were randomly selected to receive C1-inh injections or vehicle injections. Rats were given subcutaneous (s.c.) injections of C1-inh (20 U/kg) 4, 24, and 48 hours after the onset of SE.

Open Field (OF)

As a measure of recovery time, an open field test was done 3 days after SE. Rats were placed in a square test chamber (62X62X46 cm) for twenty minutes under red light and recorded from above. Any-maze software was used to quantify measures of motility (e.g. distance travelled, velocity) and anxiety (e.g. inner duration, freezing).

Novel Object Recognition (NOR) Test

The NOR test was used to assess hippocampal-dependent recognition memory in SE and SE+C1-Inh rats and sham-treated control rats. The protocol for NOR was modified from a previous study (Brewster et al., 2013). Rats were handled every day by experimenters for one week before behavioral testing began to allow the rats to acclimate to being handled. Behavioral testing began two weeks after the episode of SE. Before any behavioral testing, rats were acclimated to the central room of the suite for 30 minutes in single housed cages. Twenty-four hours prior to NOR, rats were habituated to the test chamber (62X62X46 cm) for 20 minutes. Habituation was recorded and used as an open field (OF) test for motility and anxiety. Any-maze software was used to score total distance traveled, average velocity, freezing, and percent time in the “inner zone.” The following day, rats were placed back in the testing chamber for five minutes and allowed to explore two identical objects, placed in opposite and symmetrical locations. After a two hour retention period, one of the objects was replaced with a novel object and the rats were allowed to explore for 5 minutes. The placement of the novel object was counterbalanced to control for side preference. Rats were placed facing the wall of the test chamber halfway between both objects to avoid any preference. Test chamber and objects were thoroughly cleaned with 70% ethanol between each trial. Exploration of the familiar and novel objects (defined by rats coming in contact with the objects, or < 1cm from the objects) was scored with Any-maze software, verified by hand scoring, and analyzed using paired t tests.

Barnes Maze (BM)

Twenty-four hours after NOR rats were tested for spatial memory using the BM test (Levin et al., 2012; Locklear & Kritzer, 2014). The maze consisted of a black circular platform (1.22 m diameter) elevated 1.68 meters with 18 equally spaced holes (10.16 cm diameter) along the outer edges. The maze contained a removable escape box. Visual cues for navigation were placed on all walls (triangles, squares, etc.). Thirty minutes prior to BM all rats were single housed and acclimated in the adjacent room in the dark as bright light was used to create an anxiogenic condition during testing. Twenty-four hours before testing, rats were habituated to the table in red light conditions. All rats were first trained to find the hidden escape box in three steps, in which they were allowed to remain in the box undisturbed for 2 minutes, each separated by 15 minutes: (1) rats were placed directly into the escape box; (2) rats were placed on the maze surface adjacent to the escape box and allowed to enter the box or gently guided into it; (3) the rats were placed on a temporarily constructed walkway leading from the center of the maze to the escape box. If the rats did not immediately walk towards the box they were gently guided into it. A single fruit loop was placed inside the escape box during habituation to provide a reward for entering the box. Training took place throughout the following 4 days with 4 trials per day separated by 15 min. The location of the escape box was rotated 180˚ from habituation. After acclimation, rats were placed in the center of the maze in an opaque start box. After a 10 second delay, bright lights were turned on and the start box was lifted. Rats were given up to 3 minutes to enter

the escape box or guided to it if they did not find it on their own. Once in the escape box rats were allowed to remain there for one minute. Latency to find the escape box was measured. The probe trial took place on the fifth day. All holes were covered and rats were given 90 seconds to explore the maze then returned to their home cages. Any-maze was used to determine the percent time spent directly on top of hole which previously contained the escape box (the target). Throughout testing, the maze was thoroughly cleaned with 70% ethanol and rotated to eliminate odor trails. The escape box was always in the same spatial location.

Immunohistochemistry

Rats were deeply anesthetized with beuthenasia and perfused with ice cold 1X phosphate buffered saline (PBS; 137 mM NaCl, 2.7 mM KCl, 4.3 mM Na_2HPO_4, 1.47 mM KH_2PO_4, pH 7.4) followed by ice cold 4% paraformaldehyde (PFA). Brains were quickly dissected and post fixed in 4% PFA overnight. After cryoprotection in 30% sucrose, brains were frozen in pre-chilled isopentane and stored at -80˚C until ready to use. Serial sections were taken at 30-50µm using a Leica CM1860 cryostat and stored in 1XPBS + 0.1% sodium azide. We used serial sections along the dorsoventral axis at approximately the following Bregma coordinates: -3.00mm, -3.48 mm, -4.08 mm, -4.36 mm, -4.92 mm, and -5.28 mm. These sections represent an equal sampling of the hippocampus along its dorsoventral axis. IHC was done in free floating sections. After a 5 minute (min) wash in 1XPBS, sections were incubated in hydrogen peroxide for 30 min followed by a 20 min wash in

1XPBS with 3% triton (T). Then brain sections were incubated in immunobuffer (5% goat serum, 0.3% BSA, 0.3% triton diluted in 1XPBS) for 1-24 hrs followed by a 24-48 hr incubation in primary antibody. Primary antibodies used include mouse anti-Map2, mouse anti-NeuN (1:3K; Millipore, Temecula, CA); rabbit anti-IBA1 (1:3K; Wako, Cambridge, MA); and rabbit anti-C1q (1:200; Abcam, Cambridge, MA). Following incubation in primary antibody, sections were washed with 1XPBS+0.1%T and incubated with goat anti-mouse or anti-rabbit secondary antibodies for a minimum of 1 hr at room temperature (RT). Then sections were incubated in avidin-biotin complex solution (ABC) diluted in 1XPBS for 30 min before being put in 3,3'-Diaminobenzidine (DAB) peroxidase substrate solution following manufacturer instructions in order to produce a brown stain indicating immunoreactivity. Stained sections were mounted on gelatin covered slides, stained with cresyl violet, dehydrated in increasing concentrations of ethanol (50%-100%), de-fatted in xylene, and coverslipped using permount mounting medium. For colocalization studies with IF, biotinylated primary antibodies were used for Map2 and C1q and secondary antibodies conjugated with Alexa Fluor (405-647) were used. Sections were mounted on slides, air-dried, and coverslipped with Dako fluorescent mounting medium (Dako, Carpinteria, CA, USA). Immunoreactivity was visualized using a fluorescence microscope (Leica DM5500) followed by deconvolution processing for Z stacks.

Semi-Quantitative Densitometry Analysis

Imaging of immunostained brain sections was done with Leica DM500 microscope and images were captured with high resolution digital camera (Leica MC120 HD) with 4X objectives using the LAS4.4 software. Relative mean pixel intensity was measured blinded to treatment group using Image J NIH software (V1.49). Densitometry analyses were performed bilaterally over the dorso-ventral axis of the hippocampus. Brain tissues that were damaged and the hippocampal anatomical landmarks were broken and thereby unrecognizable following the free-floating IHC procedures were excluded from the quantitative analyses. Therefore, between 4 and 6 sections were analyzed per brain.

Western Blot

Rats were deeply anesthetized and perfused with ice cold 1XPBS. Hippocampi were rapidly dissected and stored in -80˚C until ready to use. Hippocampi were homogenized in ice-cold homogenization buffer (1XPBS containing 0.2% protease inhibitor cocktail). Bradford Protein Assay (Bio Rad, Hercules, CA, USA) was used to determine protein concentration. Samples were normalized and diluted in Laemmli loading buffer (4X: 0.25 M Tris, pH 6.8, 6% SDS, 40% sucrose, 0.04% Bromophenol Blue, 200 mM Dithiothreitol). After SDS-PAGE proteins were transferred to polyvinylidene fluoride (PVDF) membranes. Membranes were incubated in blocking solution (5% non-fat milk diluted in 1X Tris Buffered Saline) with 0.1% tween (T) for one hour at room temperature. Then, membranes were incubated overnight at 4˚C in primary

antibody diluted in blocking solution. The primary antibodies used include goat anti-C3 (1:500; MP Biomedical (Cappel), Solon, OH) and rabbit anti-actin (1:5000; Sigma-Aldrich, St. Louis, MO). Following incubation with primary antibodies membranes were washed in 1X TBS-T (3x5 min). Membranes were then incubated for one hour at RT with secondary antibodies labeled with horseradish peroxidase: anti-rabbit IgG (1:5000; Vector Laboratories, Burlingame, CA) or anti-goat IgG (1:5000; ThermoFisher Scientific, Rockford, IL). Membranes were then washed in 1X TBS-T (3x5 min) and incubated with enhanced chemiluminescence (ECL) prime western blotting detection reagent (GE Healthcare, Buckinghamshire, UK). Immunoreactive bands were captured on autoradiography film. Films were developed and scanned for densitometry analysis. Some membranes were stripped from primary antibodies by incubating in stripping buffer (25 mM glycine, pH 2.0, 10% SDS) for 1-2 hours at RT. Membranes were then washed in 1X TBS-T (3x10 min), blocked, and re-incubated with different primary antibodies.

Western Blot Analysis

Optical density of immunoreactive bands was measured using Image J NIH software (V1.49). Optical densities obtained for all bands of interest were normalized for loading to the actin levels within the same lane. All groups were normalized to the average of the control group.

Golgi Staining

Rats were profoundly anesthetized with Beuthanasia and perfused with ice cold 1XPBS. All brains were rapidly dissected and processed using the FD

Rapid Golgi Stain kit following the manufacturer's instructions (Neurodigitech, San Diego, CA, USA). Brains were incubated in Golgi impregnating solutions provided in the kit for 4 weeks. Brains were cut into serial coronal sections (80 µm), mounted on gelatin-coated slides, and stained following the FD Rapid Golgi Stain kit protocol. After staining, sections were dehydrated through increasing alcohol concentrations [50%, 70%, 95%, 100%], de-fatted in Xylene, and coverslipped using Permount mounting media. Spine density was quantified using a 100X immersion (oil) objective with a Leica DM5500 microscope equipped with a high definition Leica DFC290 camera and with the LASV4.6 software. Five representative sections were selected along the dorsoventral axis at approximately the following Bregma coordinates: -3.48 mm, -4.08 mm, -4.36 mm, -4.92 mm, and -5.28 mm. Five CA1 neurons were randomly selected per section. From these, the number of spines was counted in 20 µm sections of five second order dendrites per neuron as previously described (Brewster et al., 2013). Total dendritic branches analyzed per group: Control: 375; 3 day post-SE: 375; 14 days post-SE: 375; 35 days post-SE: 240. Brains per group: Controls: 3; 3 day post-SE: 3; 14 days post-SE: 3; 35 days post-SE: 2.

Statistical Analysis

GraphPad Prism 6 software was used for statistical analyses and Analysis of Variance (ANOVA) with Tukey's post hoc test to determine statistical significance ($\alpha < 0.05$) between the control and experimental groups.

Values are reported as means ± SEM. Figures were generated using Adobe Photoshop (CS6).

RESULTS

SE Triggers a Transient Decrease in Map2 Immunoreactivity in the CA1 Hippocampal Area

We determined the temporal progression in the distribution of Map2 immunostaining in the mature hippocampal formation at 4 hrs, 1-, 3-, 14-, and 35- days after an episode of pilocarpine-induced SE (Fig. 1). Densitometry analysis followed by ANOVA revealed significant group effects for the intensity of Map2 IR signal in the CA1 pyramidal cell layer (pcl) and stratum radiatum (sr) [CA1 pcl, $F(6, 39) = 6.40$, $p < 0.001$; CA1 sr, $F(6, 39) = 6.12$, $p < 0.001$], as well as the molecular layer (ml) of the Dentate Gyrus (DG) [DG ml, $F(6, 39) = 3.35$, $p < 0.01$] (Fig. 1I). In contrast, the intensity of Map2 IR localized in the CA3 region was not significantly altered by SE [4 hrs to 35 days (d)] when compared to the control group (CA3 pcl [$F(6, 39) = 1.74$, $p = 0.13$], CA3 sr [$F(6, 39) = 1.26$, $p = 0.30$]). In control hippocampi, a homogenous distribution of Map2 IR was evident throughout the dendritic fields of CA1-3 sr (Fig.1A). High magnification images of the CA1 area showed a continuous Map2 staining pattern within the labeled dendritic structures of control hippocampi (Fig. 1A). At 4 hrs-1 d post-SE, the intensity of Map2 IR over the CA1 pcl and sr regions was comparable to that of the control group ($p > 0.05$) (Fig. 1B-C). Between 3

Figure 1. Temporal profile of Map2 immunostaining in the hippocampus after status epilepticus (SE). A, shows a representative image of the Map2 staining (brown) from a control hippocampus with a high magnification image of the CA1 area (boxed). B-H show representative hippocampal images with high magnification of boxed CA1 areas at different time points after an episode of SE (B, 4 hrs; C, 1 day (d); D, 3d; E-F, 14d; H, 35d). A representative image of a hippocampus from a rat that was given pilocarpine but failed to develop SE (pilo-non SE; Pilo in graphs) is shown in G. I, shows the densitometry analysis as relative mean pixel intensity for the different hippocampal sub-regions CA1 pyramidal cell layer (pcl) and stratum radiatum (sr), CA3 pcl and sr, and the molecular layer (ml) of the dentate gyrus (DG). Note that significant differences in the intensity of Map2 immunoreactivity are evident within the CA1 region between the control group and 1-35d post-SE groups. Data are shown as mean ± standard error of the mean. *, $p < 0.05$; **, $p < 0.01$; ***, $p < 0.001$ compared to the control group. #, $p < 0.05$, comparison between 14d and 35d groups (n = 3-9/group) (shown inside the bar graphs). ANOVA with Tukey's post hoc test.

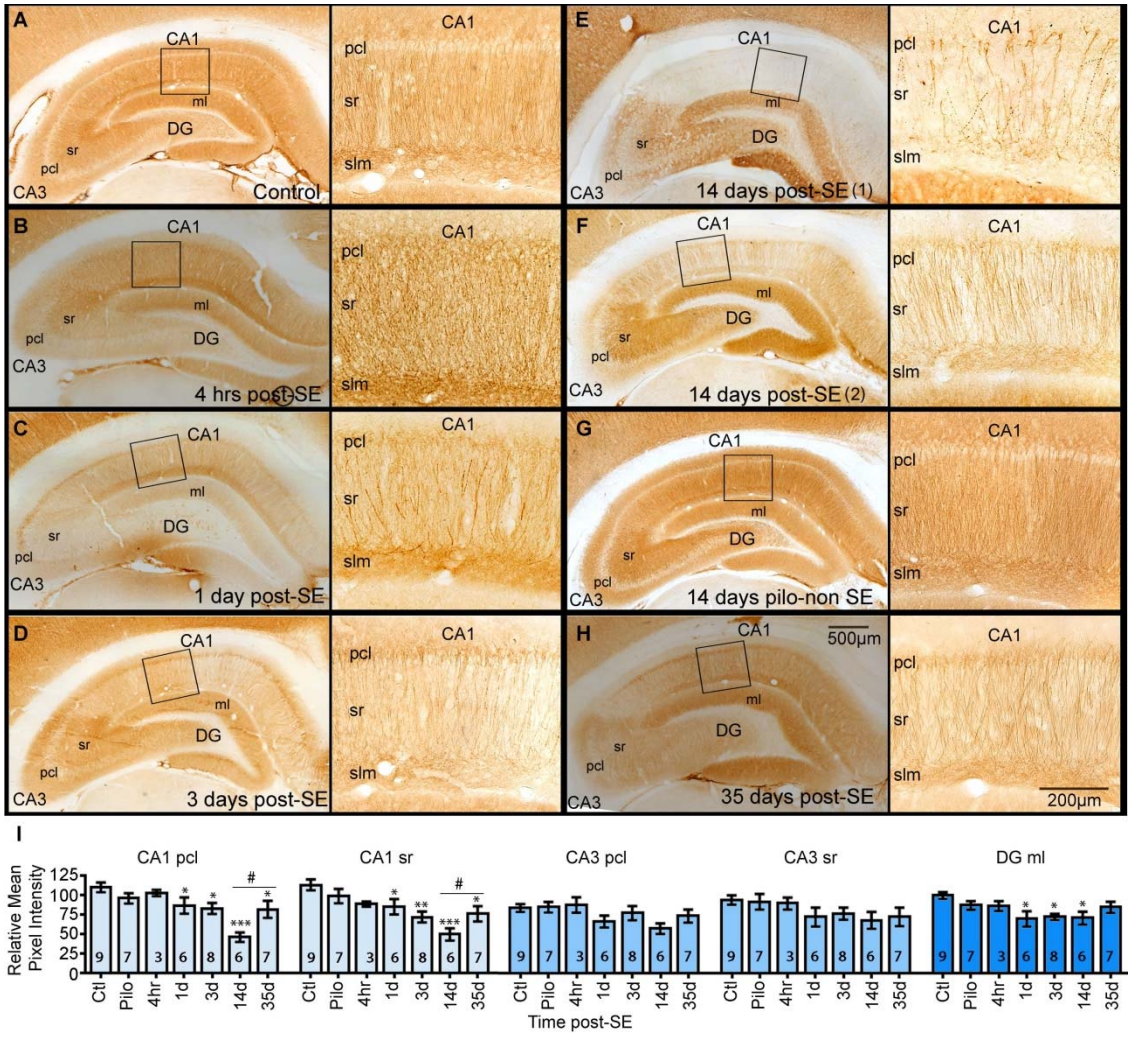
A
Control
B
4 hrs post-SE
C
1 day post-SE
D
3 days post-SE
E
14 days post-SE (1)
F
14 days post-SE (2)
G
14 days pilo-non SE
H
35 days post-SE
500µm
200µm
CA1
CA3
DG
ml
sr
pcl
slm
I
CA1 pcl
CA1 sr
CA3 pcl
CA3 sr
DG ml
Relative Mean Pixel Intensity
Ctl
Pilo
4hr
1d
3d
14d
35d
Time post-SE

and 14 days post-SE, the Map2 signal was gradually and significantly less intense than the control group in the CA1 sr (ctl vs 3d, $p < 0.01$; ctl vs 14d, $p < 0.001$) region and significantly less intense in the CA1 pcl region at 14 days compared to control ($p < 0.001$) (Fig. 1D-F).

Note that a number of dendrites displayed prominent punctated Map2 staining by day 14. The significant decrease in Map2 IR in the CA1 area seen at two weeks post-SE was specific to the SE event. Rats that received the same dose of pilocarpine but did not develop class 5 seizures showed a hippocampal distribution of Map2 similar to controls (14 days pilo-non SE; Fig. 1G) ($p > 0.05$). At 35 days following SE onset, the Map2 IR levels in CA1 pcl were significantly decreased compared to controls ($p < 0.01$) (Fig. 1H) and resembled that observed at 1-3 days post-SE ($p > 0.05$). However, a significant increase in the intensity of Map2 IR was observed between 14 and 35 days after SE ($p < 0.01$) suggesting a partial recovery of Map2 IR in the CA1 region.

To determine whether dendritic arborizations were present in the CA1 region at the time points when Map2 was significantly decreased, we performed Golgi staining in controls and at 3-, 14- and 35-days post-SE (Fig. 2). While Golgi impregnation was evident throughout all hippocampal regions, the structural analysis of dendritic arborizations was largely obstructed by the presence of Golgi impregnated glial cells in all SE groups. Thus, we quantified the spine density of second order CA1 dendritic branches and performed an ANOVA to determine a group effect [$F(3, 1361) = 10.01$, $p < 0.001$]. We found that in parallel to Map2 decline, spine density was significantly decreased at

Figure 2. Temporal profile of changes in spine density in hippocampal CA1 cells after status epilepticus (SE). A-D, shows representative images of golgi impregnated hippocampal dendrites from a control rat (A) and at different time points following an episode of SE (B, 3 days (d); C, 14d; D, 35d). E, shows representative images of 20 µm sections of CA1 dendritic branches from a control, and 3-, 14- and 35- days post-SE. F, shows the quantitative analysis of spine density in all groups. Data are shown as mean ± standard error of the mean. *, $p < 0.05$; ***, $p < 0.001$ compared to the control group. N numbers of dendritic branches quantified per animal are shown inside the bar graphs. ANOVA with Tukey's post hoc test.

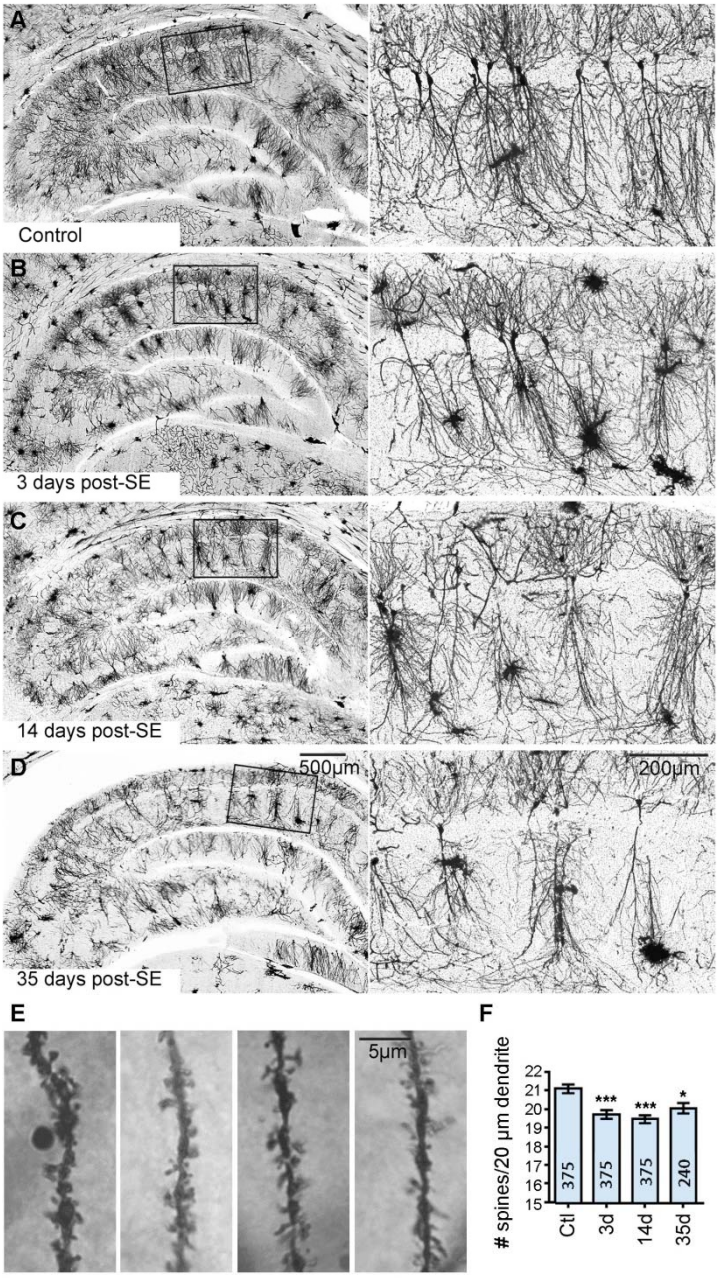
A
Control
B
3 days post-SE
C
14 days post-SE
D
35 days post-SE
500µm
200µm
E
5µm
F
spines/20 µm dendrite
22
21
20
19
18
17
16
15
375
375
375
240
***
***
*
Ctl
3d
14d
35d

3-, 14- and 35-days post-SE when compared to the control group (ctl vs 3d, $p < 0.001$; ctl vs 14d, $p < 0.001$; ctl vs 35d, $p < 0.05$).

SE Triggers a Transient Increase in Microgliosis That is Prominent in the CA1 Region

We previously showed that Map2 loss in the CA1 area correlated with accumulation of hypertrophied microglia at 2 and 3 weeks after SE (Brewster et al., 2013). However, little is known about the temporal progression between these events in the same tissues. Therefore, in parallel to Map2 and in consecutive brain sections, we mapped the temporal profile of SE-induced microglial changes in the hippocampus using IBA1 to identify these cells (Fig. 3). Densitometry analysis of IBA1 signal followed by ANOVA showed a significant group effect in areas CA1, CA3 and hilus [CA1, $F(6, 43) = 14.71$, $p < 0.001$; CA3, $F(6, 42) = 5.81$, $p < 0.001$; hilus, $F(6, 42) = 6.22$, $p < 0.001$] (Fig. 3I). In the control group, immunostaining showed a homogeneous distribution of IBA1-positive microglial cells throughout the hippocampal regions CA1, CA3, and DG (Fig. 3A). Higher magnification images from the CA1, CA3, and DG areas showed that in control hippocampi the morphological features of microglial cells included small cell bodies with highly branched and elongated processes (Fig. 3A, arrows). We found that SE triggered changes in the morphology and accumulation of IBA1-stained microglial cells in the hippocampus that progressed between 4 hrs and 35 days (Fig.3B-H). Four hrs after SE onset, the processes of microglial cells localized throughout all hippocampal regions (CA1, CA3 and DG) were hypertrophied compared to

Figure 3. Temporal profile of IBA1 immunostaining in the hippocampus after status epilepticus (SE). A-H, show representative images of the IBA1 staining (brown) from a control hippocampus (A) and from hippocampi collected at different time points after an episode of SE (B, 4 hrs; C, 1 day (d); D, 3d; E-F, 14d; H, 35d). A representative hippocampus from a rat that was given pilocarpine but failed to develop SE (pilo-non SE; Pilo in graphs) is shown in G. Right panels show high magnification images of boxed CA1, CA3, and the hilus of the dentate gyrus (DG). High magnification images with IBA1-labeled microglia (arrows) are also shown. Nissl stained cellular nuclei are shown in blue. Abbreviations: pcl, pyramidal cell layer; sr, stratum radiatum; slm, stratum lacunosum-moleculare. I, shows the densitometry analysis as relative mean pixel intensity for the different hippocampal sub-regions CA1, CA3, and hilus. Significant differences in the intensity of IBA1-stained microglia are evident in the CA1, CA3, and hilar regions at 4 hrs and 14d after SE compared to the control group. Data are shown as mean ± standard error of the mean. *, $p < 0.05$; **, $p < 0.01$; ***, $p < 0.001$ compared to the control group. #, $p < 0.05$, comparison between 14d and 35d groups (n = 4-11/group) (shown inside the bar graphs). ANOVA with Tukey's post hoc test.

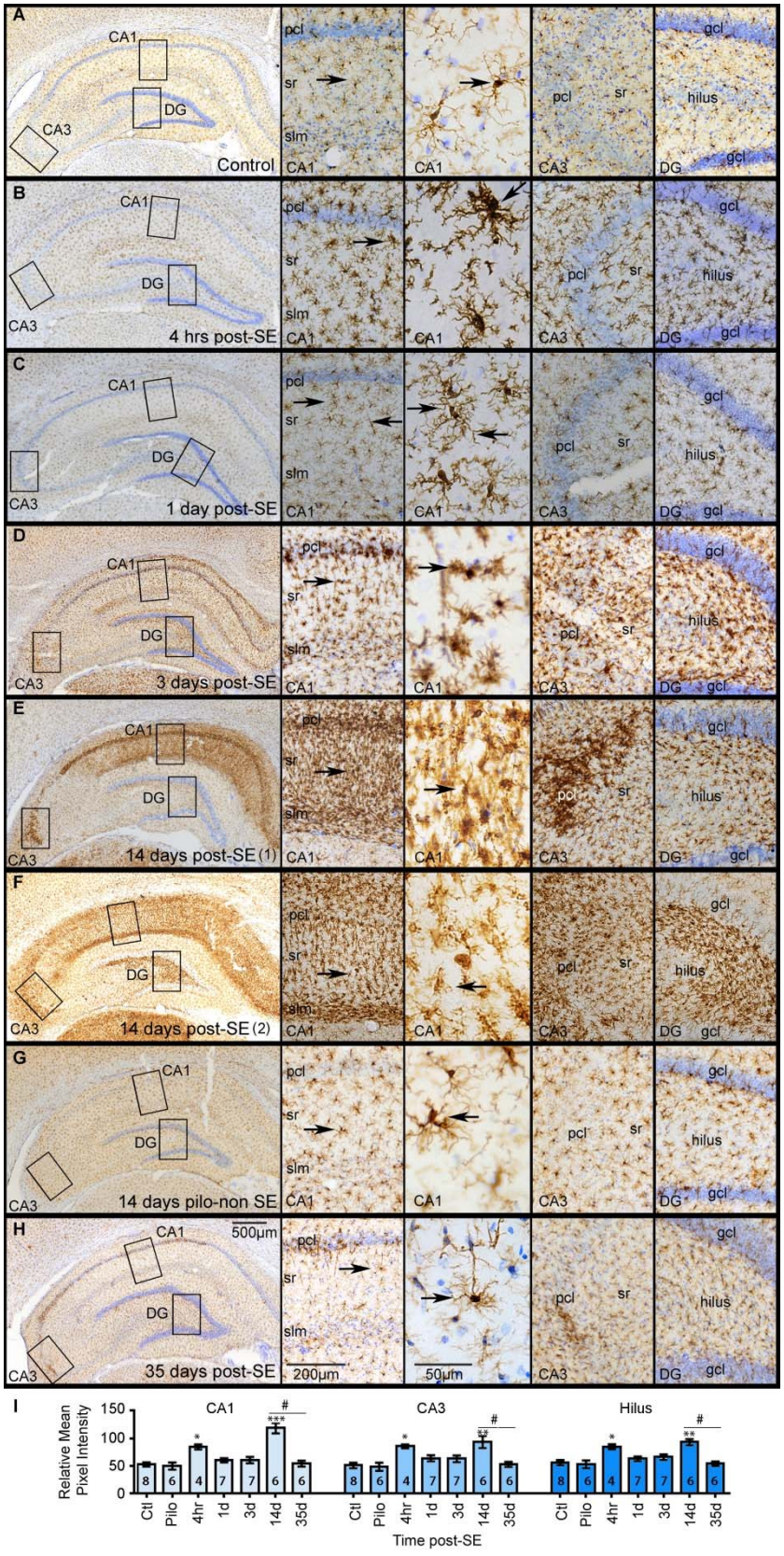
A
CA1
DG
CA3
Control
pcl
sr
slm
gcl
hilus
B
4 hrs post-SE
C
1 day post-SE
D
3 days post-SE
E
14 days post-SE (1)
F
14 days post-SE (2)
G
14 days pilo-non SE
H
500µm
35 days post-SE
200µm
50µm
I
Relative Mean Pixel Intensity
CA1
CA3
Hilus
Ctl
Pilo
4hr
1d
3d
14d
35d
Time post-SE

those of control hippocampi. Furthermore, the levels of IBA1 IR at 4 hrs after SE were significantly increased throughout all hippocampal regions compared to the control group (CA1, $p < 0.05$; CA3, $p < 0.05$; hilus, $p < 0.05$). By day 1 after SE, the morphology of microglial cells and IBA1 IR levels were similar to the control group ($p > 0.05$) (Fig. 3C). At 3 days post-SE, drastic changes were evident in the morphology of microglial cells from highly branched to amoeboid (Fig. 3D). Throughout the hippocampus, smaller amoeboid microglia displayed shortened processes at 3 days after SE compared to the earlier time points and to the control group (Fig. 3A-D). By two weeks post-SE, a robust immunostaining for IBA1-positive amoeboid microglia was concentrated within the pcl, sr, and slm of the CA1 region (Fig. 3E-F). At this time point the presence of amoeboid microglia also was evident in the CA3 pcl and in the hilar region of DG, albeit at a lesser extent to that observed in the entire CA1 area. Statistical analyses showed a significant increase in the intensity of IBA1 IR at 14 days post-SE compared to the control group in all hippocampal regions (CA1, $p < 0.001$; CA3, $p < 0.01$; DG, $p < 0.01$). The intensity of IBA1 signal in the 14 day pilo-non SE group was not different from controls in all hippocampal areas ($p > 0.05$) (Fig. 3G). Furthermore, we found that the drastic SE-induced changes on microglial morphology and accumulation in the CA1 hippocampus were nearly resolved by 35 days after SE (Fig. 3H). Note that at this time point IBA1 IR was significantly less intense when compared to the 14 day post SE-time point in all hippocampal regions (CA1, $p < 0.01$; CA3, $p < 0.01$; DG, $p < 0.01$) and not significantly different to controls ($p > 0.05$).

SE Triggers a Transient Increase in the Classical Complement Component C1q in the CA1 Stratum Radiatum Hippocampal Subregion

Previous studies demonstrated that proteins of the classical complement pathway, which is initiated by C1q, can tag neuronal elements for microglia to recognize and eliminate (Schafer et al., 2012). For instance, C1q and its downstream effector C3b are associated with the activity-dependent elimination of synapses in the normal developing brain (Stephan et al., 2012; Stevens et al., 2007). Enhanced attraction and contacts between microglial processes and CA1 dendrites occur following SE (Brewster et al., 2013; Eyo et al., 2014; Hasegawa et al., 2007). However, the functional significance of these contacts is not known. Thus, we investigated whether C1q and C3 proteins from the classical complement pathway were altered after SE. First, we determined the distribution of C1q in the CA1 region of the hippocampus (Fig. 4), where substantial loss of Map2 and accumulation of IBA1-positive microglia were observed (Figs. 1, 3) (Brewster et al., 2013; Schartz et al., 2016). We focused on the time points in which significant changes in Map2 and IBA1 were observed (3-35 d) and performed IHC with antibodies against C1q. In the control group, immunostaining showed a distribution of C1q (Fig. 4A) that was mainly localized to the slm of the CA1 region. In contrast, after SE the IR signal for C1q appeared throughout the CA1 pcl, sr and slm regions (Fig. 4B-4E). Densitometry analysis of C1q IR followed by ANOVA showed no overall group differences between control hippocampi and hippocampi taken at 3-, 14-, 25-, or 35-days after SE in the pcl [$F(5, 31) = 1.76$, $p = 0.16$] or the sr [$F(5, 31) =$

Figure 4. Temporal profile of C1q immunostaining in the hippocampus after status epilepticus (SE). A-E, show representative images of the C1q staining (brown) from a control hippocampus (A) and from hippocampi collected at different time points after an episode of SE (B, 3 days (d); C, 14d; D, 23d; E, 35d). Nissl stained cellular nuclei are shown in blue. F, shows the densitometry analysis as relative mean pixel intensity for hippocampal subregions CA1 pyramidal cell layer (pcl) and stratum radiatum (sr). Significant differences in the intensity of C1q immunoreactivity are evident in the CA1 sr subregion at 14d after SE compared to the control group. G, shows colocalization of C1q (green) with Map2 (red), in control CA1 hippocampi and in hippocampi from 3-, and 14-days after SE. Note that due to the low intensity of Map2 IR at 14 days, potential colocalization with C1q is inconclusive. Data are shown as mean +/- standard error of the mean. N numbers of animals used are shown inside the bar graphs. *, $p < 0.05$. ANOVA with Tukey's post hoc test.

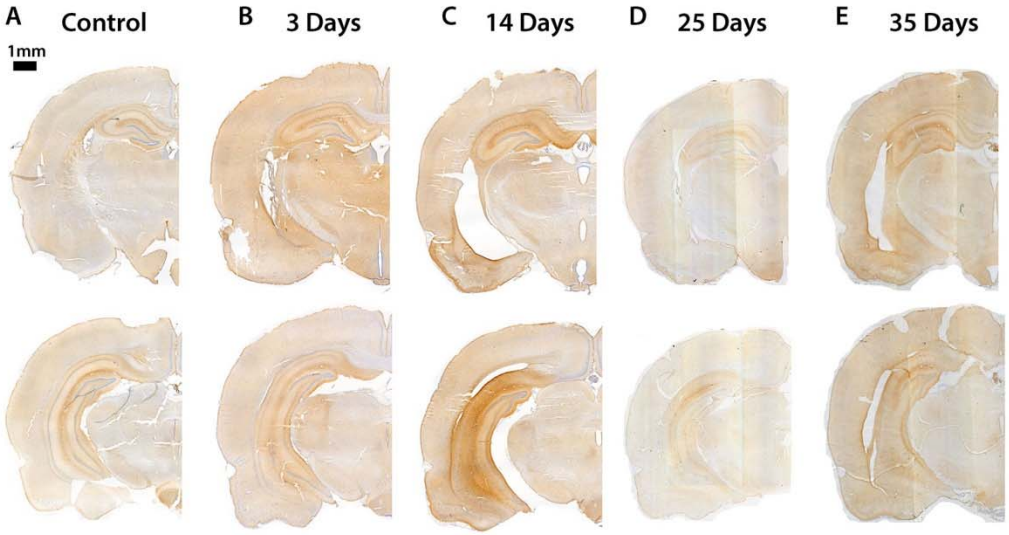
A
Control
B
3 Days
C
14 Days
D
25 Days
E
35 Days
1mm

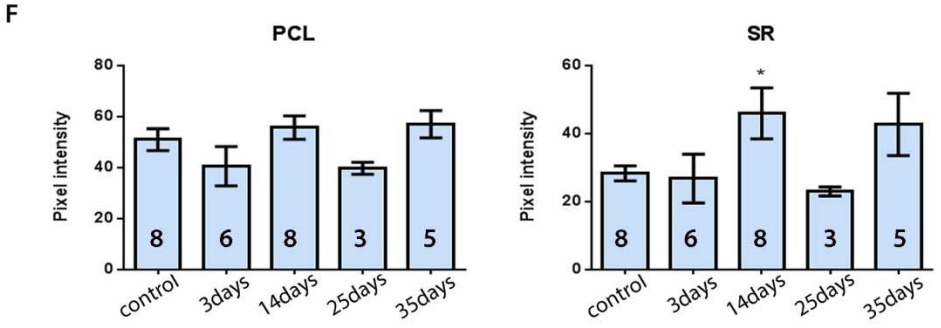
F
PCL
SR
Pixel intensity
80
60
40
20
0
8
6
8
3
5
control
3days
14days
25days
35days
*

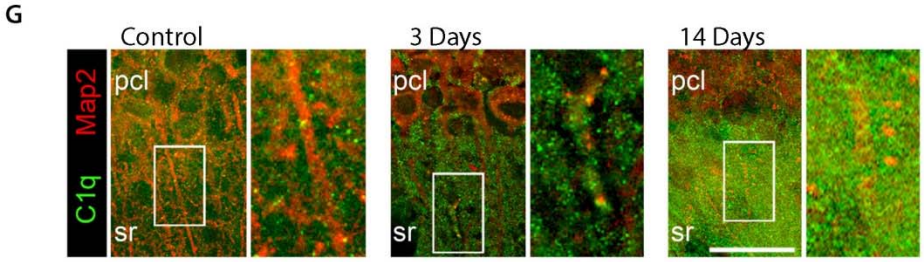
G
Control
3 Days
14 Days
Map2
C1q
pcl
sr

2.15, $p = 0.08$] of the CA1 hippocampus (Fig. 4F). However, since the most drastic changes in microglia and Map2 IR are observed at 14 days after SE, we directly compared C1q IR in control hippocampi and hippocampi from 14 days post-SE. An unpaired T test revealed a significant increase in C1q IR in the sr of the CA1 region 14 days after SE when compared to the control [$t(14) = 2.25$, $p < 0.05$].

SE Triggers a Transient Increase in C3 and Its Cleavage Products in the Hippocampus

Complement protein C3 is activated downstream of C1q. Upon activation, C3 is cleaved into its biologically active products C3a and C3b. C3a is released and works to attract microglia to the site of interest and C3b works to opsonize cells, cellular structures, or debris for microglia to engulf and eliminate (Stephan et al., 2012). We used western blotting to quantify the cleavage of C3 in whole hippocampal homogenates from different time points after SE (14, 21 and 35 days) and compared them to age matched controls (Fig. 5). Note that commercially available antibodies for C3b with rat specificity were not available for our histological studies; therefore we used an antibody against all C3 forms for western blotting. Figure 5A shows a representative western blot including several time points (14-35 d) next to age matched control samples. The immunoblot shows an overall increase in C3 protein levels in all the SE groups as compared with the respective controls. We analyzed the western blots with a series of unpaired t tests of the SE and control matched time points for three different immunoreactive bands

Figure 5. Temporal profile of C3 protein levels and cleavage after an episode of status epilepticus (SE). A, shows representative western blot of C3 in hippocampi dissected at different time-points (14-, and 25-, and 35-days) after SE loaded next to respective age-matched controls. Different bands represent cleavage products of C3: C3bα, C3bβ, and iC3b. Below is the same blot immunoblotted with actin, the loading control. B, shows the densitometry analysis as percent pixel intensity for C3bα, C3bβ (C), and iC3b (D). All experimental time points were compared to their corresponding controls. Data are shown as mean +/- standard error of the mean. N numbers of animals used are shown inside bar graphs. *, $p < 0.05$, #, $p = 0.06$. Unpaired t test. ANOVA with Tukey's post hoc test.

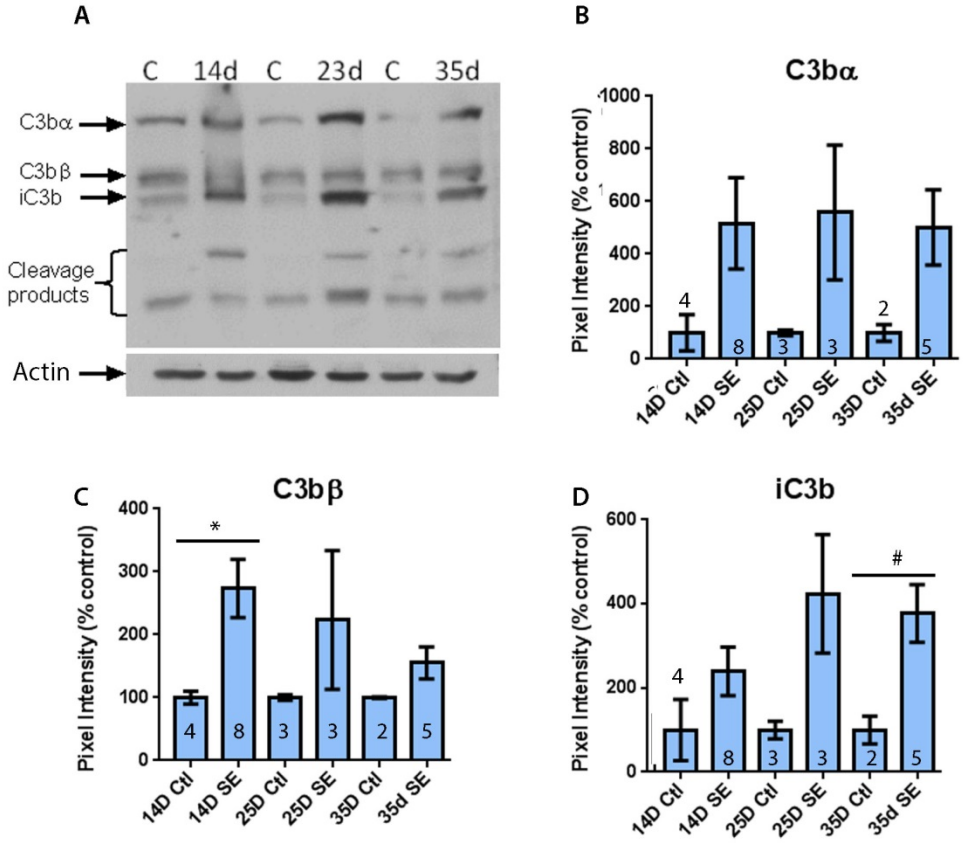
A
C
14d
C
23d
C
35d
C3bα
C3bβ
iC3b
Cleavage products
Actin
B
C3bα
Pixel Intensity (% control)
1000
800
600
400
200
0
4
8
3
3
2
5
14D Ctl
14D SE
25D Ctl
25D SE
35D Ctl
35d SE
C
C3bβ
Pixel Intensity (% control)
400
300
200
100
0
*
4
8
3
3
2
5
14D Ctl
14D SE
25D Ctl
25D SE
35D Ctl
35d SE
D
iC3b
Pixel Intensity (% control)
600
400
200
0
#
4
8
3
3
2
5
14D Ctl
14D SE
25D Ctl
25D SE
35D Ctl
35d SE

representing C3bα, C3bβ, and iC3b. Densitometry analysis revealed a significant increase in the protein levels of C3bβ at 14 days after SE when compared to controls [$t(10) = 2.56$, $p < 0.05$]. Furthermore, there was a trend for an increase in levels of iC3b at 35 days post SE when compared to their age matched controls [$t(5) = 2.39$, $p = 0.06$]. Increasing the sample size at later time points may provide more definitive information about levels of C3 after SE.

Because complement activation after SE occurs at the same time points as the drop in Map2 and the peak of microgliosis, we hypothesized that the classical complement pathway may be driving the microglia-mediated dendritic alterations. In addition, because it is likely that these alterations in the hippocampus are driving cognitive deficits observed in models of SE (Brewster et al., 2013; Pearson et al., 2014), inhibiting this pathway may attenuate dendritic alterations and associated behavioral deficits. We therefore used C1-Inh to block activation of the classical complement pathway immediately after SE and evaluated the time-course of microgliosis and dendritic alterations, along with cognitive function as measured with tests such as NOR and BM (Fig. 6).

Acute Treatment With C1-Inh Does not Attenuate Map2 Loss in the CA1 Region of the Hippocampus

Since aberrant activation of the classical complement pathway coincides with dendritic alterations after SE, we used a pharmacological approach to inhibit complement activation via the classical pathway immediately following SE to determine its role in SE-induced microgliosis and dendritic alterations.

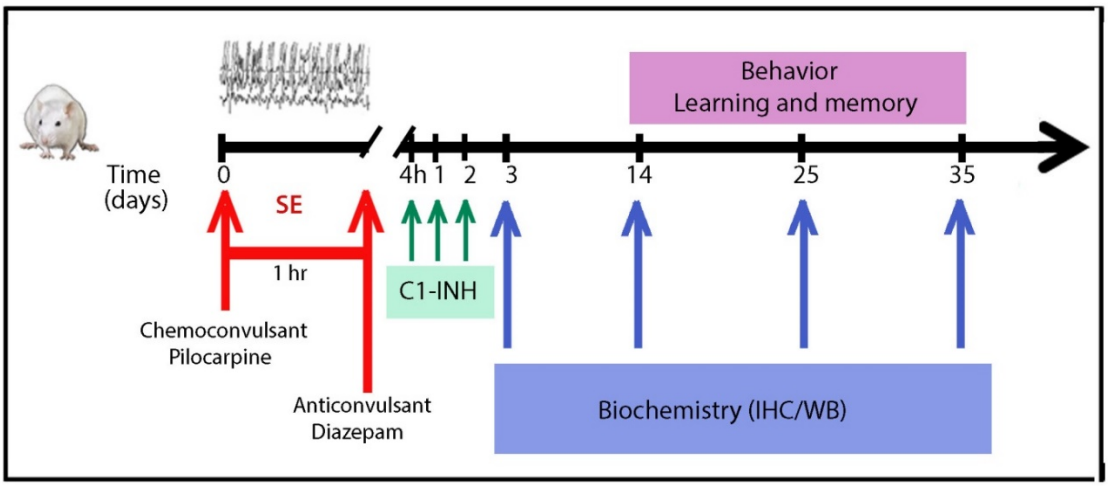

Figure 6. Experimental paradigm for treatment with C1-esterase inhibitor (C1-Inh) after status epilepticus (SE). The timeline of SE induction (day 0), C1-Inh treatment (20U/kg, s.c; days 0, 1, and 2), tissue collection (days 3, 14, 25, and 35), and behavioral testing [open field (OF), novel object recognition (NOR), and Barnes maze (BM) (days 14-23)].

C1-inh was administered subcutaneously at 4-, 24-, and 48-hrs after SE and tissue was collected at 3-, 14-, and 25-days after SE and processed for IHC with antibodies against Map2 (Fig.7). Map2 IR within the CA1 hippocampal region was quantified using densitometry analysis and compared to the control and experimental tissue from the time course analysis of Map2 (Fig. 1). Figure 7A shows a representative control section stained for Map2. There is homogenous distribution of Map2 throughout the dorso-ventral axis of the hippocampus. Figures 7B-D show the time course of Map2 distribution in SE and SE+C1-Inh with representative dorsal and ventral sections at 3-, 14-, and 25-days after SE. Densitometry analysis revealed a reduction in Map2 IR at all time points after SE (Fig. 7E) when compared to the control group [$F(3, 35) = 16.76$, $p < 0.001$]. Map2 IR levels in the SE+C1-Inh groups were significantly reduced when compared to the control group [$F(3, 27) = 12.36$, $p < 0.001$]. Interestingly, we found that C1-Inh administered to SE rats did not attenuate the SE-induced reduction of Map2 IR in the hippocampal CA1 region. Significant differences were not evident at 3, 14 or 25 days in the SE+C1-inh group compared to the respective SE groups.

Acute Treatment With C1-Inh Exacerbates Accumulation of Microglia to the CA1 Region of the Hippocampus

We next sought to determine if treatment with C1-Inh after an episode of SE could prevent the aberrant accumulation and activation of microglia. Activation of the classical pathway C1q-C3 produced biologically active peptides that serve various functions including recruitment of microglia and

Figure 7. C1-esterase inhibitor (C1-Inh) treatment does not attenuate Map2 loss in CA1 hippocampus after an episode of status epilepticus (SE). A, shows a representative image of the Map2 staining (brown) from a control brain. B-D, show representative brain images at different time points after an episode of SE, next to an image from matching time-points after SE with C1-Inh treatment (B, 3 days (d); C, 14d; D, 25d). E, shows the densitometry analysis of Map2 immunoreactivity (IR) as percent control pixel intensity for the hippocampal CA1 region. Note that Map2 IR is lowest at 14d after SE, and is not altered with C1-Inh treatment compared to SE. Data are shown as mean ± standard error of the mean. N numbers of animals used are shown inside bar graphs. **, $p < 0.01$; ***, $p < 0.001$ compared to the control group ($n = 4–20$/group). ANOVA with Tukey's post hoc test.

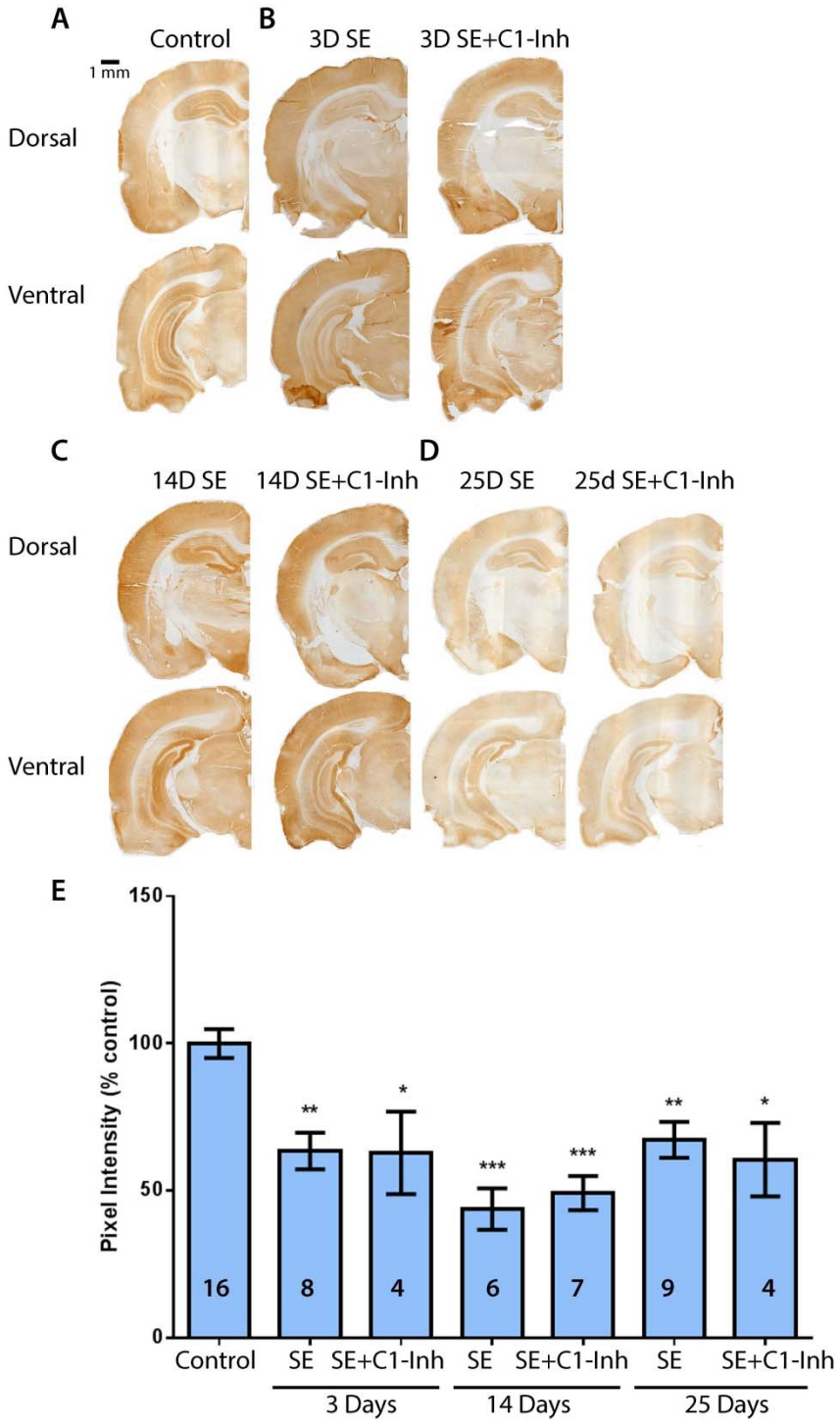
A
Control
B
3D SE
3D SE+C1-Inh
1 mm
Dorsal
Ventral
C
14D SE
14D SE+C1-Inh
D
25D SE
25d SE+C1-Inh
Dorsal
Ventral
E
Pixel Intensity (% control)
150
100
50
0
**
*
***
***
**
*
16
8
4
6
7
9
4
Control
SE
SE+C1-Inh
SE
SE+C1-Inh
SE
SE+C1-Inh
3 Days
14 Days
25 Days

macrophages and promote inflammation, in addition to the eat me signals C1q and C3b (Stephan et al., 2012).

Tissue collected at 3-, 14-, and 25-days after SE with C1-Inh treatment was immunostained with antibodies against IBA1 (brown), a marker for microglia, and IR signal was quantified with densitometry analysis (Fig. 8). We compared the SE+C1-Inh group with the time-matched SE and control samples. Densitometry analysis was restricted to the CA1 region of the hippocampus where substantial microgliosis was previously observed after SE (Fig. 3) (Brewster et al., 2013; Schartz et al., 2016). Figure 8A shows a representative control section stained for IBA1. There is light homogenous distribution of IBA1 throughout the dorso-ventral axis of the control hippocampus. Figures 8B-D show the time course of IBA1 distribution in SE and SE+C1-Inh with representative dorsal and ventral sections at 3-, 14-, and 25-days after SE. ANOVA revealed a significant group effect on the levels of IBA1 IR across the groups [$F(6, 51) = 20.34$, $p < 0.001$]. Specifically, post hoc analysis showed that there was a significant increase in IBA1 IR levels in the CA1 hippocampus at 3 days in the SE+ C1-Inh group when compared to control samples ($p < 0.01$) whereas no difference was observed between the control group and SE group at 3 days after SE (Fig. 3). Additionally, the IR levels of IBA1 were significantly higher at in the SE+C1-Inh groups (14 and 25 days) in comparison to the control samples (Fig. 8E) (ctl vs 14d SE+C1-Inh, $p < 0.001$; ctl vs 25d SE+C1-Inh, $p < 0.001$). Interestingly, IBA1 IR levels were also significantly higher in the SE+C1-inh groups when compared to the SE

Figure 8. C1-esterase inhibitor (C1-Inh) exacerbates microgliosis in the CA1 hippocampus after status epilepticus (SE). A, shows a representative image of the IBA1 staining (brown) from a control brain. B-D, show representative brain images at different time points after an episode of SE, next to an image of a matching time-point after SE with C1-Inh treatment (B, 3 days (d); C, 14d; D, 25d). E, shows the densitometry analysis of IBA1 immunoreactivity (IR) as percent control pixel intensity for the hippocampal CA1 region. Note that significant differences in the intensity of IBA1 IR are evident at 3 days after SE with C1-Inh treatment and persist up to 25 days, whereas without C1-Inh treatment IBA1 immunoreactivity peaks at 14 days and decreases thereafter. Data are shown as mean ± standard error of the mean. N numbers of animals used are shown inside bar graphs. *, $p < 0.05$; ***, $p < 0.001$. ##, $p < 0.01$; ###, $p < 0.001$ compared to the control group ($n = 4–20$/group). ANOVA with Tukey's post hoc test.

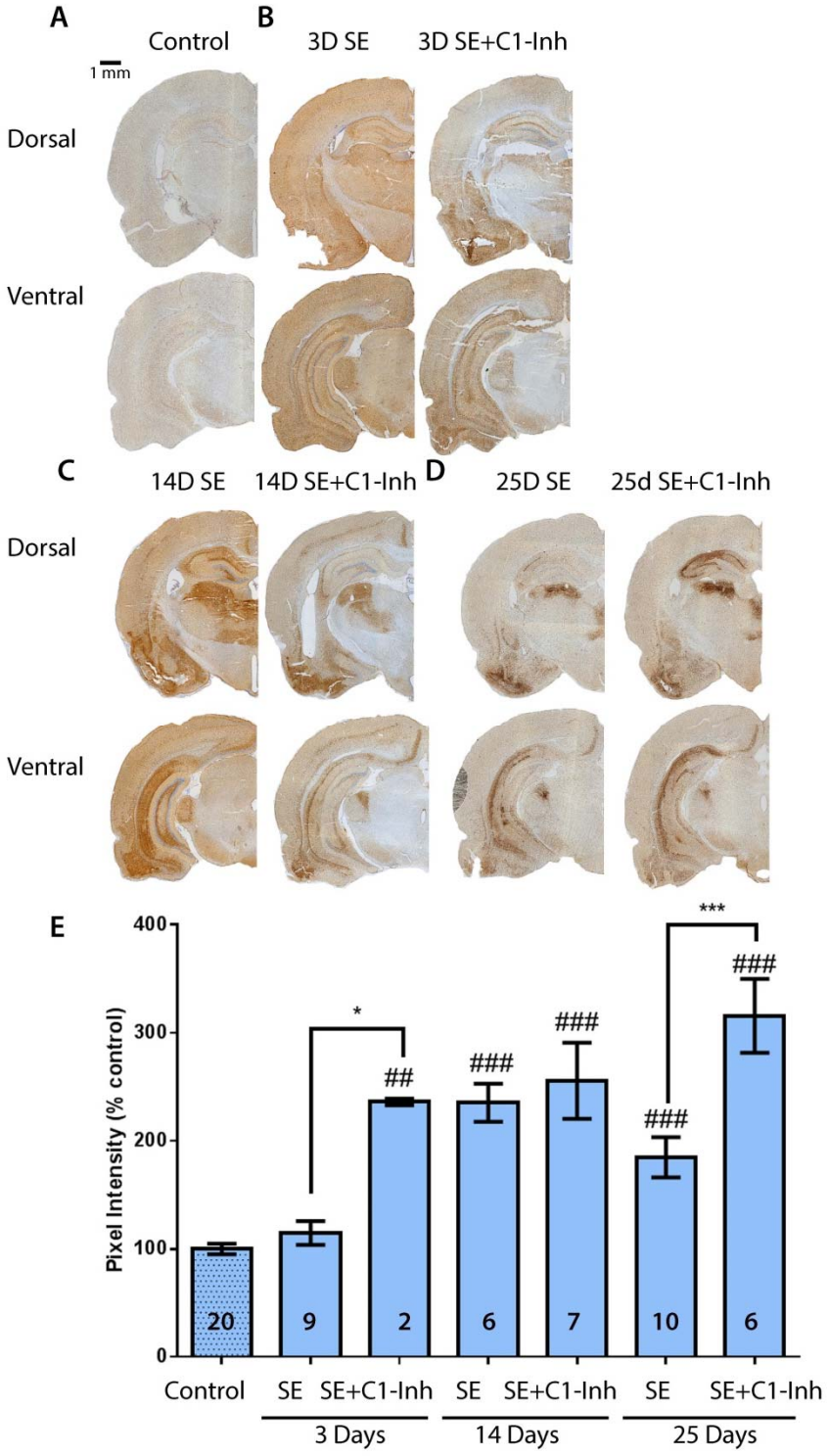
A
Control
B
3D SE
3D SE+C1-Inh
1 mm
Dorsal
Ventral
C
14D SE
14D SE+C1-Inh
D
25D SE
25d SE+C1-Inh
Dorsal
Ventral
E
Pixel Intensity (% control)
400
300
200
100
0
*
***
##
###
###
###
###
20
9
2
6
7
10
6
Control
SE
SE+C1-Inh
SE
SE+C1-Inh
SE
SE+C1-Inh
3 Days
14 Days
25 Days

group [$F(5, 32) = 8.41$, $p < 0.001$]. Taken together these data suggest that acute treatment with C1-Inh may exacerbate SE-induced microgliosis in the hippocampus.

Cognitive deficits are often comorbid in humans with TLE; these observations are replicated in experimental models of SE and acquired TLE (Brewster et al., 2013; Chauviere et al., 2009; Jacobs et al., 2009; Lesting, Geiger, Narayanan, Pape, & Seidenbecher, 2011; Levin et al., 2012; Muller, Bankstahl, Groticke, & Loscher, 2009; Nolan et al., 2003; Pearson et al., 2014; Swann & Hablitz, 2000; Szyndler et al., 2005; Wong, 2005). Interestingly, cognitive and behavioral impairments observed in epilepsy are often common with those seen in Alzheimer's disease (Chin & Scharfman, 2013). This is important because aberrant levels of complement transcripts are found in human TLE (Aronica et al., 2007) and also in Alzheimer's disease (reviewed in (Kolev et al., 2009)) and thus suggest a role for aberrant complement system activation in the mechanisms underlying cognitive disturbances. Building upon these studies and our findings that increased protein levels of C1q and cleavage of C3 occur after SE (Figs. 4, 5) we hypothesized that a SE-induced aberrant activation of the complement system may increase the risk of hippocampal-dependent memory deficits and that inhibition of the classical complement signaling with C1-Inh may attenuate this pathophysiology.

Motility and Anxiety-Like Behaviors are not Altered Following SE or C1-Inh Treatment

As a control for future behavioral studies, we evaluated the in the locomotion of all rats (controls, SE and SE+C1-Inh rats) using the open field test. Experiments were done at 14 days following SE. Rats were placed in an open square testing arena in the dark for 20 minutes and the following measures were analyzed: total distance travelled, average velocity, percent of time spent in the inner portion of the arena, and percent time freezing (Fig. 9).

An analysis of measures of motility revealed no overall group effect on distance travelled [$F(2, 46) = 1.79$, $p = 0.18$] or velocity [$F(2, 46) = 1.79$, $p = 0.18$] (Fig. 9A-B). Interestingly, an unpaired t test revealed that the SE group covered more distance than the control group [$t(35) = 2.15$, $p < 0.05$]. This finding is indicative of hyperactivity associated with epilepsy and potentially ADHD (Ramos, Carreiro, Scorza, & Cysneiros, 2016). However, because our ANOVA was not significant, more precise measures are needed to further explore this effect. We also analyzed measures of anxiety-like behavior with ANOVA and found no group effect of time spent in the inner portion of the open field arena [$F(2, 46) = 1.77$, $p = 0.18$] or percent of time freezing [$F(2, 46) = 1.46$, $p = 0.24$]. The time spent in the inner portion of the arena can be associated with decreased anxiety, because the rats would spend more time along the tall walls of the arena if anxiety levels were increased. More time freezing would be indicative of increased anxiety, as rats have an instinctual response to freeze in situations perceived as dangerous.

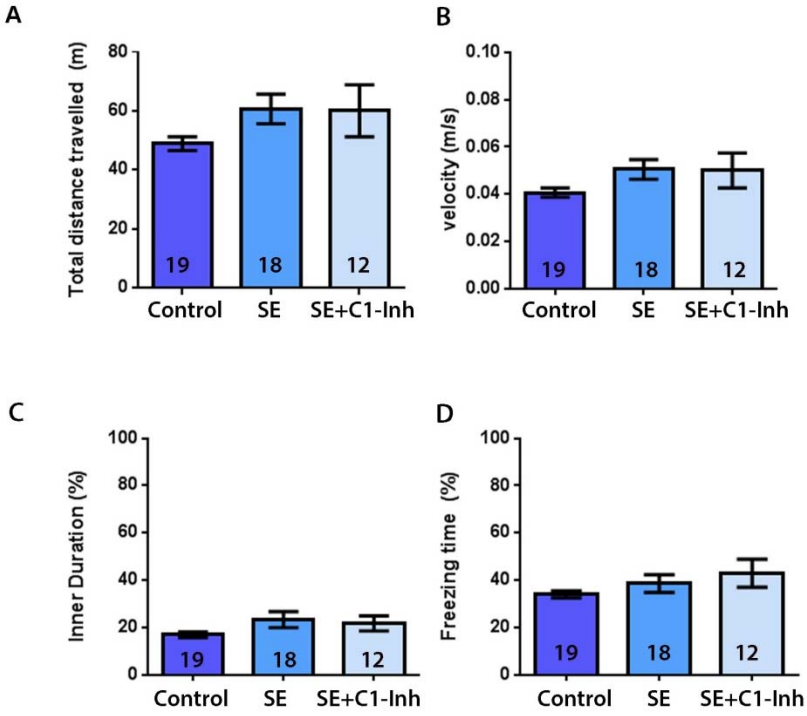

Figure 9. Status epilepticus (SE) does not alter behavior in the open field test. Open field test was done at 14 days after SE on control rats, and those exposed to SE with and without the C1 esterase inhibitor treatment (C1-Inh). The distance traveled (a) and velocity (b), were not different between the groups. Similarly, measures of anxiety such as time spent in the center of the testing arena (c) or amount of freezing (d) were not changed. No significant differences were found (*n* = 12-19/group). N numbers of animals used are shown the inside bar graphs. Data are shown as mean +/- standard error of the mean. ANOVA with Tukey's post hoc test.

Note that this test was also performed at 3 days post SE (Fig. 10). No differences between groups were observed [distance, $F(2, 15) = 0.37$, $p = 0.69$; velocity $F(2, 15) = 0.36$, $p = 0.70$; inner duration, $F(2, 15) = 1.23$, $p = 0.32$; freezing, $F(2, 15) = 0.20$, $p = 0.82$]. Taken together these data suggest that at 3 days after SE there are no deficits in locomotion across the groups while at 14 days a trend for deficits starts to become evident. Future studies will determine whether locomotion and anxiety are altered at later time points, as epileptogenesis progresses in this model of acquired TLE.

Recognition Memory Deficits are not Attenuated With C1-Inh Treatment Following SE

To identify potential SE-induced changes in hippocampal-dependent memory function we used the NOR test. Specifically, the NOR test was used to measure changes in recognition memory after SE and SE with C1-inh treatment relative to age-matched controls (Fig. 11). Testing was done at 2 weeks after SE because previous studies have confirmed that a deficit occurs at this time after SE (Brewster et al., 2013) and paralleled the histopathological changes (Figs. 1-3). During the first trial, rats were given 5 minutes to explore two identical objects under red light. The percent time spent with each object was measured (Fig. 11A). A paired t test showed no preference for either the left or right object in any group [control, $t(20) = 0.21$, $p = 0.83$; SE $t(20) = 0.44$, $p = 0.66$; SE+C1-inh, $t(10) = 0.31$, $p = 0.76$]. After a two hour delay, rats were placed back in the testing arena with one previously explored ‘familiar’ object and one of the objects replaced with a new ‘novel’ object (Fig. 11B). Control

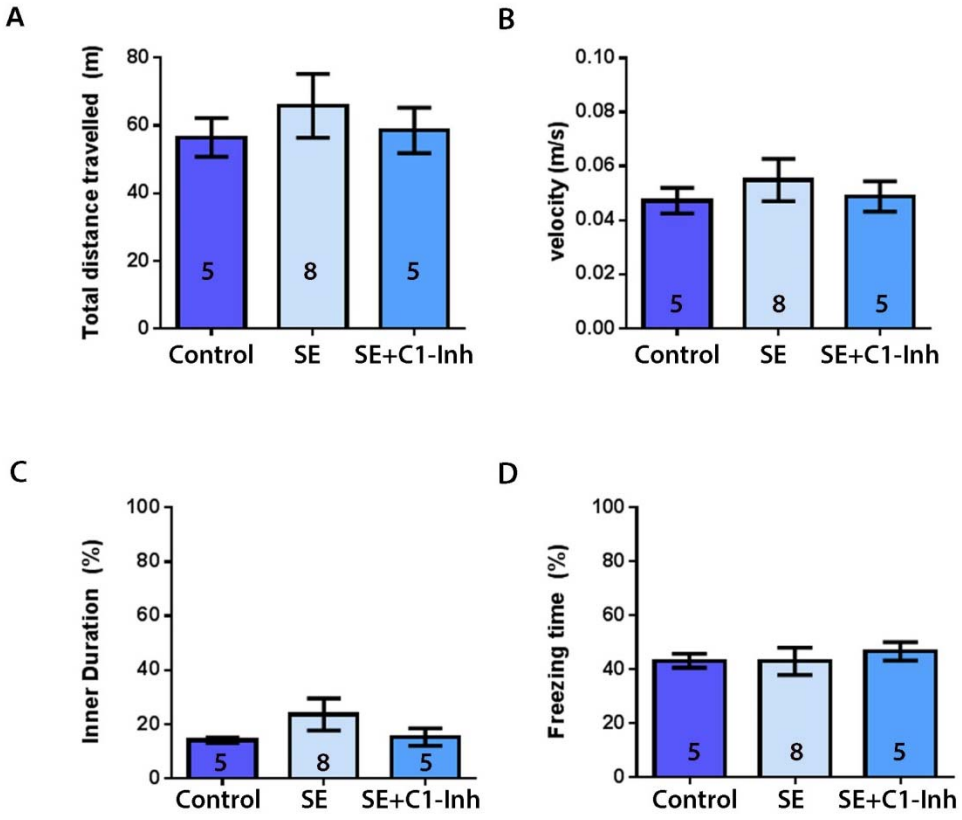

Figure 10. Open field test 3 days after an episode of SE. Three days after SE, rats were tested in an open field paradigm to detect differences in recovery between control, SE, and SE+C1-Inh groups. The distance traveled (a) and velocity (b), were not different between the groups. Similarly, measures of anxiety such as time spent in the center of the testing arena (c) or amount of freezing (d) were not changed. No significant differences were found (*n* = 12-19/group). N numbers of animals used are shown the inside bar graphs. Data are shown as mean +/- standard error of the mean. ANOVA with Tukey's post hoc test.

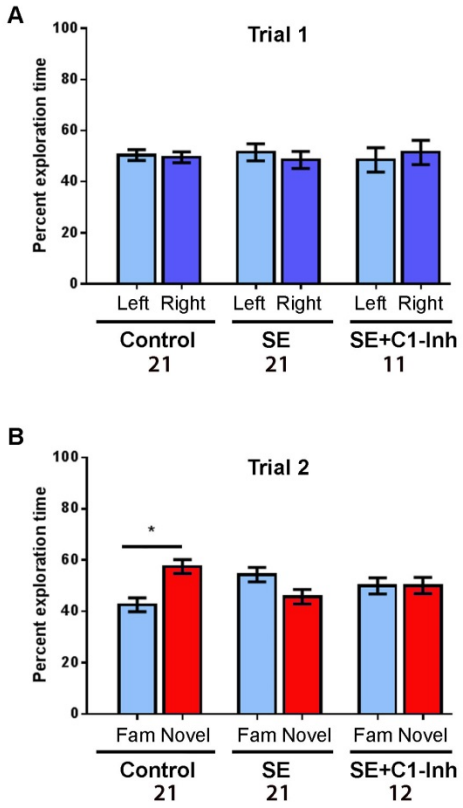

Figure 11. Treatment with C1-esterase inhibitor (C1-Inh) does not attenuate recognition memory in rats subjected to status epilepticus (SE). The novel object recognition (NOR) test was used to measure recognition memory after SE and after SE with C1-Inh treatment. A, shows the percent exploration time of each object during the first trial. None of the treatment groups showed preference for either the right or the left object. B, shows the percent exploration time during the second trial. Note that only the control animals showed any preference towards the novel object, thus recognition of the familiar object. Data are shown as mean +/- standard error of the mean. *, $p < 0.05$ (n = 11-21/group). N numbers of animals used are shown inside bar graphs. ANOVA with Tukey's post hoc test.

rats spent more time exploring the novel object [$t(20) = 2.77$, $p = 0.01$] suggesting they remembered the familiar object from the previous trial. However, both the SE and SE+C1-inh rats spent an equal amount of time exploring the novel and familiar objects. Lack of exploratory preference toward the novel object suggests failure to recognize the familiar object in the SE and SE+C1-Inh groups [SE, $t(20) = 1.53$, $p = 0.14$; SE+C1-inh, $t(11) = 0.02$, $p = 0.98$] and thereby suggesting a memory deficit. Of importance, an ANOVA showed no differences in total exploration time between the control group and the experimental groups in either NOR trial 1[$F(2, 50) = 0.38$, $p = 0.68$] or NOR trial 2 [$F(2, 50) = 0.20$, $p = 0.82$.

Hippocampal-Dependent Spatial Memory Deficits Induced by SE are not Attenuated With C1-Inh

The Barnes maze (BM) test was used to assess changes in hippocampal-dependent spatial memory after SE and SE with C1-inh treatment relative to age-matched controls. ANOVA was used to compare performance (measured by latency to find the escape box) over 4 days of training between groups (Fig. 12A). There was a significant effect of treatment [$F(2, 120) = 40.89$, $p < 0.001$], revealing a deficit in experimental rats throughout BM training. On the first training day, no significant differences were observed in mean latencies for finding the escape box (ctl = 74.62 ± 12.07s; SE = 94.98 ± 8.39s; SE+C1-Inh = 113.40 ± 15.43s). On the second training day, SE+C1-Inh rats (M = 115.70 ± 18.21s) performed worse than control rats (M = 34.46 ± 12.45s,) $p < 0.001$) and worse than SE rats (M = 60.33 ± 7.72s,$p < 0.01$),

*Figure 12***.** Treatment with C1-esterase inhibitor (C1-Inh) does not attenuate spatial memory in rats subjected to status epilepticus (SE). Barnes Maze (BM) was used to assess spatial memory after SE and after SE with C1-Inh treatment. A, the rats were trained over 4 days (4 trials per day) to find an escape hole on a circular table with “false holes.” The graph shows the latency to find and enter the escape box during the training period. Data are shown as mean +/- standard error of the mean. *, $p < 0.05$; **, $p < 0.01$; ***, $p < 0.001$ compared with control. B, Probe trial measuring time spent over the covered escape box (s). Data are shown as mean +/- standard error of the mean. *, $p < 0.05$ compared to control group. C, shows representative tracking of the rats’ movements during the probe trial. (n = 8-13/group). ANOVA with Tukey’s post hoc test.

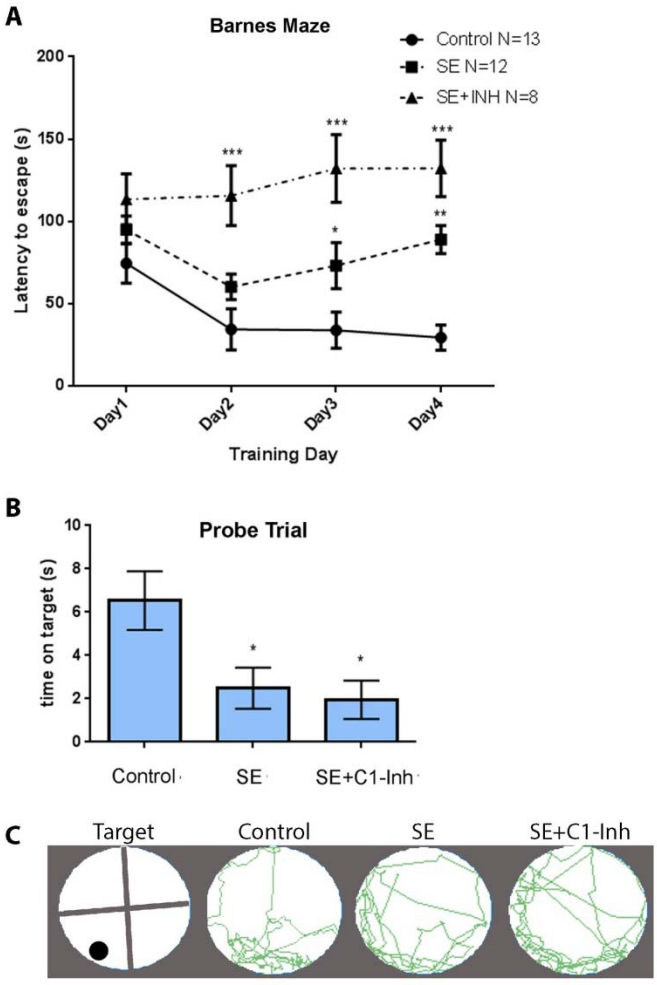
A
Barnes Maze
Control N=13
SE N=12
SE+INH N=8
Latency to escape (s)
200
150
100
50
0
***
***
***
*
**
Day1
Day2
Day3
Day4
Training Day
B
Probe Trial
time on target (s)
10
8
6
4
2
0
*
*
Control
SE
SE+C1-Inh
C
Target
Control
SE
SE+C1-Inh

taking longer than both groups to find the escape box.) On day three, both SE and SE+C1-Inh groups showed a deficit in finding the escape box as compared to control [ctl vs. SE, $p < 0.05$; ctl vs SE+C1-inh, $p < 0.001$]. On average it took 73.25 ± 14.00 seconds and 132.2 ± 20.57 seconds for the SE and SE+C1-Inh groups to find the escape box, compared to 33.96 ± 11.00 seconds from the control group. Surprisingly, the deficit of the SE+C1-Inh group was greater than the SE group ($p < 0.01$) at this point. On the fourth and last day of training, the deficit was still present in the SE (M = 89.04 ± 8.45s) and SE+C1-inh (M = 132.30 ± 17.13s) groups when compared to controls (M = 29.50 ± 7.66s) (control vs. SE, $p < 0.01$; control vs SE+C1-Inh, $p < 0.001$). These data support the presence of a significant and persistent spatial learning deficit in rats that have had an episode of SE even with C1-inh treatment.

Twenty-four hours after the last training session, rats were placed back on the BM table for a probe trial in which the escape hole was covered. Rats were allowed to explore the maze for 90 seconds and the amount of time spent directly on top of the hole that previously contained the escape box (the target) was measured and compared between groups (Fig. 12B). An ANOVA revealed a group effect in amount of time spent on top of the target [$F(2, 30) = 4.83$, $p < 0.05$]. Specifically, post hoc tests showed that the control group spent significantly more time on top of the target than the SE ($p < 0.05$) or SE+C1-Inh ($p < 0.05$) groups suggesting a deficit in memory retention in both experimental groups. Figure 12C shows representative tracking during the probe trial for control, SE, and SE+C1-Inh rats. Although all three groups spent more time in

the quadrant that contained the target, the control groups spent more time directly on top of the target than the SE and SE+C1-Inh groups. These results indicate that SE results in a deficit in both spatial learning and spatial memory, and this deficit is not diminished with treatment with C1-Inh.

DISCUSSION

The first aim of this study describes the spatial and temporal correlation between the SE-induced changes in Map2 IR, microglial accumulation, and activation of the complement pathway in the hippocampal formation at various time points following an episode of SE. Specifically, we found that, (1) SE triggered a decline in Map2 IR in the CA1 hippocampal pcl and sr areas that was evident as early as 1 day after SE, reached minimal expression at 14 days, and was partially increased by day 35 post-SE (Fig. 1); (2) SE induced changes in the morphology of microglial cells that were evident as early as 4 hrs post-SE in all hippocampal regions; however, at 2 weeks post-SE maximal accumulation of hypertrophied/amoeboid microglia was evident mainly within the CA1 area from where it declined thereafter (Fig. 3); and (3) Proteins of the classical complement cascade increase in the hippocampus at 14 days after SE (Figs. 4, 5) which corresponds to the peak loss of Map2 and accumulation of microglia. Even though alterations in Map2 and microglia within the hippocampal formation are often seen subsequent to SE and in epilepsy (Avignone et al., 2008; Ballough et al., 1995; Brewster et al., 2013; Choi & Koh, 2008; De Simoni et al., 2000; Jalava et al., 2007; Ravizza et al., 2005; Rizzi et al., 2003; Shapiro et al., 2008; Vezzani & Granata, 2005), and complement

mRNA have been shown to be altered after SE (Aronica et al., 2007), this study is the first to describe that the evolution of these events follow similar spatial and temporal profiles in a model of SE and acquired temporal lobe epilepsy. Furthermore, this study is the first to describe temporal changes of the classical complement pathway after an episode of SE in parallel to dendritic structural alterations and microgliosis.

Spatiotemporal analyses of SE-induced Map2 changes in the hippocampus have been previously reported in the developing brain (Jalava et al., 2007). SE in the immature brain triggers transient increase in the high molecular weight Map2 protein, which is the dominant Map2 isoform in the adult brain (Jalava et al., 2007; Sanchez, Diaz-Nido, & Avila, 2000). In contrast, we found that SE in the mature brain triggers a decline in Map2 IR that is more prominent in the CA1 hippocampal region (Fig. 1). First, we observed that the extent to which Map2 IR was decreased in CA1 pcl and sr was similar suggesting a global reduction of Map2 protein in CA1 cells. This could be due to alterations in the activation of intracellular signaling cascades such as mTOR and/or MAPK/ERK pathways which have been shown to regulate protein synthesis of Map2 and also are altered by SE (Brewster et al., 2013; Gong & Tang, 2006; Lugo et al., 2008).

Map2 loss in the hippocampal CA1 region may impact the morphology and stability of the dendritic structures. This is supported by studies showing that Map2 deficient mice display reduced dendritic lengths along with decreased microtubule densities (Harada et al., 2002). Map2-microtubule

stability is important for neuronal homeostasis which includes cellular processes such as protein trafficking (Dehmelt & Halpain, 2005; Gardiner, Overall, & Marc, 2011; Harada et al., 2002; Urbanska, Blazejczyk, & Jaworski, 2008). The finding that the maximal reduction in Map2 IR at two weeks after SE was no longer evident at 35 days post-SE suggests a partial recovery of Map2 IR in CA1 and thereby a transient SE-induced effect.

Furthermore, a number of studies support that when neurons are challenged with abnormal activity (i.e. seizures) their physiological responses adapt to the initial imposed changes most likely trying to restore normal activity patterns (homeostatic plasticity) (Swann & Rho, 2014). Thus, it is possible that the SE-induced transient decline of Map2 IR may be an attempt of potentially viable CA1 cells to maintain stability of their dendritic structures along with neuronal functions and thereby may be a beneficial event. However, because Map2 is critical for the stability and growth of dendritic elements (Dehmelt & Halpain, 2005; Gardiner et al., 2011; Harada et al., 2002; Urbanska et al., 2008) it is also possible that the temporary reduction of this protein directly contributes to the decline in dendritic arborization and spine densities of hippocampal CA1 cell (Wong, 2005; Wong & Guo, 2013). At the time points when Map2 IR levels were the most significantly reduced (3-35 days post-SE), we quantified the dendritic spine densities of CA1 cells and found a significant decline (Fig. 2) suggesting a correlation between these events. Nevertheless, the possibility that homeostatic mechanisms involving transcriptional, translational, or cellular transport/trafficking processes underlie changes in

Map2 levels, and whether SE-induced Map2 loss is detrimental or beneficial for viable neurons requires investigation. Taken together these data suggest that there is a spatial and temporal association between reduced Map2 levels and a decrease in spine density following pilocarpine-induced SE in the mature rat hippocampus.

It is also expected that some of the SE-induced Map2 loss is directly a consequence of neuronal death and injury (Ballough et al., 1995). We previously mapped the progression of cleaved caspase-3 after an episode of SE and found a peak in IR at 3 days post-SE (Schartz et al., 2016). The unparalleled temporal progression of maximum apoptosis with that seen for Map2 at two weeks suggests that additional mechanisms may be underlying the disruption of neuronal expression of Map2 at later time points. Interestingly, at 35-days post-SE Map2 IR levels did not recover beyond the levels seen at 3 days post-SE. These data further suggest the possibility that a large number of viable cells remain in the CA1 area even at 2 weeks post-SE. Furthermore, we found that the neuronal marker NeuN was not drastically changed after SE (Schartz et al., 2016).

Prominent microgliosis overlapped with decreased Map2 IR in CA1 sr area at 2-3 weeks post SE has been previously reported (Brewster et al., 2013). In this study we mapped the progression of these events and showed that there is considerable spatial and temporal overlap between the SE-induced loss of Map2 IR and increased microgliosis in the CA1 area. Substantial evidence support that microglia undergo inflammatory activation

after SE. Releases of a number of inflammatory mediators have been shown to contribute to some of the neuropathological changes associated with prolonged seizures (Choi & Koh, 2008; Vezzani et al., 2011). We recently confirmed neuroinflammation at the acute time points following pilocarpine-induced SE (Arisi, Foresti, Katki, & Shapiro, 2015; Benson, Manzanero, & Borges, 2015) that correlated with early changes in Map2 levels, but no significant changes in inflammatory mediators were observed at the 14 days post-SE time point when microgliosis was most prominent (Schartz et al., 2016). In addition to their inflammatory properties, microglia are phagocytic cells that clear dead cells and cellular debris along with smaller neuronal elements such as synapses (Sierra, Abiega, Shahraz, & Neumann, 2013). Thus, the vast accumulation of amoeboid microglia with shorter processes in CA1 pcl may be a related to a change to a mostly phagocytic phenotype (Kettenmann et al., 2011) which may be in response to the increased numbers of apoptotic and dead cells. Thus, it is possible that once the dead cells within CA1 have been cleared, microglial cells recede from this area over time but not before possibly potentiating dendritic alterations in the remaining viable neurons.

Recent studies show that SE enhances the attraction of microglial processes toward neural elements (Eyo et al., 2014) and increases the density of cell-to-cell contacts between activated microglia and CA1 dendrites (Brewster et al., 2013; Hasegawa et al., 2007). This is important because a growing body of evidence supports that microglial cells participate in shaping neuronal dendritic architectures and the organization of synaptic connectivity

(Paolicelli et al., 2011; Schafer et al., 2012; Tremblay et al., 2011). For instance, microglial processes regularly survey their surrounding microenvironment making direct contacts with spines and synaptic neuronal structures which they can engulf and eliminate (Nimmerjahn, Kirchhoff, & Helmchen, 2005; Paolicelli et al., 2011; Schafer et al., 2012; Tremblay et al., 2011). Thus, based on these data it is conceivable that the vast accumulation of microglial cells in CA1 may play a role in the disruption of dendritic structures probably by dysregulating Map2 in CA1 neurons.

Several studies have found an increase in the classical complement pathway in neurodegenerative or injury models (Cowell, Plane, & Silverstein, 2003; Hong et al., 2016; Silverman et al., 2016; Väkevä et al., 1994), and in epilepsy models (Aronica et al., 2007). Components of the classical complement pathway have also been shown to guide microglia to synapses and tag them for phagocytosis (Stevens et al., 2007). Thus, we hypothesized that complement proteins may be localized to areas of high microglia accumulation and loss of Map2 signal. For this reason, we mapped the distribution of C1q and the levels of C3 after SE, focusing on the time points in which Map2 and microglial changes were observed (3-35 days post-SE). We found an increase in C1q IR at two weeks post-SE that was specific to the CA1 sr (Fig. 4), which is the dendritic field of CA1 cells. This SE-induced increase in C1q IR paralleled that which was observed for the microglial marker IBA1. Given that macrophages and micorglia are known to produce and release C1q protein (Kettenmann et al., 2013), it is possible that microglia are producing

and releasing C1q. This may be underlying the increase in C1q IR seen at two weeks post SE. Moreover, we found that the C1q downstream effector C3 was cleaved, suggesting activation of C3 as an opsonin and thereby activation of the classical complement pathway (Fig. 5). This effect also peaked at 2 weeks after SE, matching the time course of C1q, microglia, and Map2 loss.

The increase in C1q and C3 proteins may result in the opsonization of neuronal elements for microglial recognition and targeting for phagocytosis. The classical complement pathway has been implicated in guiding microglia to pre- and post-synaptic structures during development. Specifically, those structures that did not form a connection were tagged by C1q and pruned by microglia (Stevens et al., 2007). Similarly, it is possible that dying or vulnerable neurons after SE result in uncoupled or weakened synapses that are then targeted by C1q for elimination by microglia. Thus, it is possible that due to cell death, which peaks at 3 days after SE (Schartz et al., 2016), some synapses are left bare or uncoupled (pre- or post-synaptic) and thereby may be tagged for elimination. However, this possibility still needs to be investigated. Taken together, these findings suggest that the classical complement pathway may be guiding microglia to stay within the sr after SE and promoting phagocytosis of tagged dendritic structures

To further understand the role of the classical complement pathway in hippocampal histopathological and functional alterations after SE, we used the C1-esterase inhibitor to block activation of this pathway immediately following SE. We measured downstream effects of complement activation such as

microgliosis to determine if treatment with C1-inh could attenuate molecular injury and behavioral deficits associated with SE. Because treatment with C1-inh has been shown to be neuroprotective after injury (Heydenreich et al., 2012), we expected treatment to be neuroprotective after an episode of SE. Surprisingly, C1-inh did not attenuate SE-induced Map2 loss in the hippocampus (Fig. 8). Map2 IR did not differ between SE and SE+C1-Inh treated rats. An unexpected finding was that treatment with C1-inh actually exacerbated microgliosis in the hippocampus, with a significant increase observed at 3 days after SE and remaining elevated up to 25 days, whereas without the treatment microgliosis peaked at 14 days and fell thereafter (Fig. 9).Therefore, it is possible that complement activation via the classical pathway is neuroprotective immediately after SE. Furthermore, because C1q levels are not elevated early on, it is possible that C1-Inh treatment immediately after SE affects normal levels of complement activation. Giving C1-Inh treatment to sham-treated rats would have provided some insight into the mechanisms affected by the drug. However, because of cost, this was not a viable option. Future studies will determine the effects of C1-Inh in control animals.

Treatment with C1-inh has been successful in attenuating injury and behavioral deficits in animal models of ischemia and stroke (De Simoni et al., 2004; De Simoni et al., 2003; Heydenreich et al., 2012), so it was expected to reduce cognitive deficits after SE. We first tested SE rats with NOR and BM and replicated previous findings (Brewster et al., 2013; Levin et al., 2012; Pearson et al., 2014) that following SE, rats exhibit recognition and spatial

memory deficits, respectively. Surprisingly, we found that treatment with C1-inh did not attenuate memory deficits, and in fact exacerbated the deficits in BM. SE rats with C1-Inh treatment performed similarly to SE rats in the NOR test (Fig. 11) and performed worse than SE rats in the BM test (Fig. 12), taking longer to learn the location of the escape box. It is known that the hippocampus is functionally differentiated, with specific regions mediating different types of memory. For instance, the dorsal hippocampus is necessary for spatial learning (Moser & Moser, 1998). In this study, we compared cellular alterations between different regions of the hippocampus (CA1, CA3, DG). However, an analysis of the alterations in the dorsal versus ventral hippocampus after SE might elucidate more localized effects of SE on the hippocampus and on memory.

In other injury models, C1-inh doses were given between 5 and 90 minutes after onset of injury, similarly to the time points of drug administration in the present study. Increased complement activation in the ischemia model has been observed within hours of injury and appears to persist for weeks (Silverman et al., 2016; Väkevä et al., 1994), whereas we saw a significant increase in C1q and C3 expression only at 2 weeks after SE. Therefore, we speculate that adjusting the time point of treatment may still be successful at preventing injury after SE if given 10-14 days after the initial episode of SE. The time course of treatment was set at 4-48 hours after SE because this is the time point in which inflammatory cytokines peaked (Schartz et al., 2016). In addition, previous studies using other immunosuppressant drugs have

demonstrated that acute treatment can be neuroprotective in models of acquired epilepsy (Brewster et al., 2013; Zeng et al., 2009).

Studies using C1-inh treatment have used intravenous (i.v) injections (De Simoni et al., 2003; Emmens et al., 2013; Heydenreich et al., 2012). Furthermore, a study compared efficacy of s.c. versus i.v. injections of C1-inh by testing serum levels at different time points after injection and found that serum levels are much higher and persist longer when given i.v. and that serum levels of C1-inh are not different from that of controls (Emmens et al., 2013). However, the literature is mixed on this topic, with results varying depending on the species used (Martinez-Saguer et al., 2014). Given this information, perhaps C1-inh treatment could attenuate deficits associated with SE if administered intravenously. We will test this possibility in future experiments.

There is also the possibility that C3 cleavage into its biologically active peptides C3a and C3b is the main cause of microgliosis and associated dendritic changes after SE. C1-inh acts both on the classical and the lectin pathways of the complement system but has no effect on the alternative pathway (Nielsen et al., 2007). It is possible that by blocking C1 esterase, cleavage of C3 is limited resulting in accumulation of C3. This could then trigger the alternative pathway of spontaneous C3 hydrolysis to cleave the C3 protein. In this case, C3 would still be cleaved into C3a and C3b, which would promote increase inflammation and phagocytosis, respectively. Further experiments are required to determine if treatment with C1-inh resulted in an

increase of C3 cleavage. Based on the behavioral and molecular results of this study, it would be expected that C3 activation is increased in the animals treated with C1-inh. Previous studies have found that deletion of complement component C3 is protective against seizures and results in improved spatial memory in models of epilepsy (Libbey et al., 2010; Perez-Alcazar et al., 2014). This would suggest that an increase in C3 cleavage may exacerbate the seizures and memory deficits in animals that sustained SE and thereby activation of the complement cascade may still be a candidate mechanism. In future experiments we may inhibit the downstream C3 molecules, which would inhibit further activation of all three complement pathways, or use mouse knockout models of the C3 ligand and receptors.

Given the number of recent studies that implicate the complement system in inflammatory pathologies it is likely that the complement system is involved in the pathology following SE. Moreover, the finding that activation of the complement pathway via the classical cascade (C1q and C3) follows the pattern of Map2 loss and microgliosis strongly suggests a role for this pathway in the remodeling observed.

Evidence for the spatiotemporal evolution of microgliosis along with the complement pathway and their association with other pathological SE-induced changes (e.g. dendritic, inflammation, astrogliosis, transcriptional/translational dysregulation) in the hippocampus is of importance when evaluating the effects of immunosuppressant and anti-inflammatory treatments in models of SE and epilepsy. For instance, early vs. late immunosuppressant treatments may lead

to different observations likely due to the temporal expression of the drug's targets in microglial cells or within the complement pathway. This may be the case underlying the unexpected findings in this study as well as the discrepant findings associated with other immunosuppressant treatments (e.g. rapamycin) in models of SE and acquired epilepsy (Brewster et al., 2013; Buckmaster & Lew, 2011; van Vliet et al., 2012; Zeng et al., 2009). Furthermore, our studies may lead to the identification of novel targets within the complement pathway to treat epilepsy and its comorbidities.

LIST OF REFERENCES

LIST OF REFERENCES

Abrahams, S., Morris, R. G., Polkey, C. E., Jarosz, J. M., Cox, T. C. S., Graves, M., & Pickering, A. (1999). Hippocampal involvement in spatial and working memory: A structural MRI analysis of patients with unilateral mesial temporal lobe sclerosis. *Brain and Cognition, 41*(1), 39-65. doi: http://dx.doi.org/10.1006/brcg.1999.1095

Aird, R. B., Venturini, A. M., & Spielman, P. M. (1967). ANtecedents of temporal lobe epilepsy. *Archives of Neurology, 16*(1), 67-73. doi: 10.1001/archneur.1967.00470190071009

Allan, S. M., & Rothwell, N. J. (2003). Inflammation in central nervous system injury. *Philosophical Transactions of the Royal Society London B Biological Sciences, 358*(1438), 1669-1677. doi: 10.1098/rstb.2003.1358

Alonso-Vanegas, M. A., Cisneros-Franco, J. M., Castillo-Montoya, C., Martínez-Rosas, A. R., Gómez-Pérez, M. E., & Rubio-Donnadieu, F. (2013). Self-reported quality of life in pharmacoresistant temporal lobe epilepsy: correlation with clinical variables and memory evaluation. *Epileptic Disorders, 15*(3), 263-271.

Amhaoul, H., Hamaide, J., Bertoglio, D., Reichel, S. N., Verhaeghe, J., Geerts, E., . . . Dedeurwaerdere, S. (2015). Brain inflammation in a chronic epilepsy model: Evolving pattern of the translocator protein during epileptogenesis. *Neurobiology of Disease, 82*, 526-539. doi: 10.1016/j.nbd.2015.09.004

Andersson, P. B., Perry, V. H., & Gordon, S. (1991). The kinetics and morphological characteristics of the macrophage-microglial response to kainic acid-induced neuronal degeneration. *Neuroscience, 42*(1), 201-214. doi: http://dx.doi.org/10.1016/0306-4522(91)90159-L

Arisi, G. M., Foresti, M. L., Katki, K., & Shapiro, L. A. (2015). Increased CCL2, CCL3, CCL5, and IL-1beta cytokine concentration in piriform cortex, hippocampus, and neocortex after pilocarpine-induced seizures. *J Neuroinflammation, 12*, 129. doi: 10.1186/s12974-015-0347-z

Aronica, E., Boer, K., van Vliet, E. A., Redeker, S., Baayen, J. C., Spliet, W. G., . . . Gorter, J. A. (2007). Complement activation in experimental and human temporal lobe epilepsy. *Neurobiology of Disease, 26*(3), 497-511. doi: 10.1016/j.nbd.2007.01.015

Avignone, E., Ulmann, L., Levavasseur, F., Rassendren, F., & Audinat, E. (2008). Status epilepticus induces a particular microglial activation state characterized by enhanced purinergic signaling. *Journal of Neuroscience, 28*(37), 9133-9144. doi: 28/37/9133 [pii]

Badawy, R. A. B., Harvey, A. S., & Macdonell, R. A. L. (2009). Cortical hyperexcitability and epileptogenesis: Understanding the mechanisms of epilepsy – Part 1. *Journal of Clinical Neuroscience, 16*(3), 355-365. doi: http://dx.doi.org/10.1016/j.jocn.2008.08.026

Ballough, G. P., Martin, L. J., Cann, F. J., Graham, J. S., Smith, C. D., Kling, C. E., . . . Filbert, M. G. (1995). Microtubule-associated protein 2 (MAP-2): a sensitive marker of seizure-related brain damage. *Journal of Neuroscience Methods, 61*(1-2), 23-32. doi: 0165-0270(95)00019-Q [pii]

Benson, M. J., Manzanero, S., & Borges, K. (2015). Complex alterations in microglial M1/M2 markers during the development of epilepsy in two mouse models. *Epilepsia, 56*(6), 895-905. doi: 10.1111/epi.12960

Berkovic, S. F., Mulley, J. C., Scheffer, I. E., & Petrou, S. (2006). Human epilepsies: Interaction of genetic and acquired factors. *Trends in Neurosciences, 29*(7), 391-397. doi: http://dx.doi.org/10.1016/j.tins.2006.05.009

Borges, K., Gearing, M., McDermott, D. L., Smith, A. B., Almonte, A. G., Wainer, B. H., & Dingledine, R. (2003). Neuronal and glial pathological changes during epileptogenesis in the mouse pilocarpine model. *Experimental Neurology, 182*(1), 21-34. doi: http://dx.doi.org/10.1016/S0014-4886(03)00086-4

Brewster, A. L., Lugo, J. N., Patil, V. V., Lee, W. L., Qian, Y., Vanegas, F., & Anderson, A. E. (2013). Rapamycin reverses status epilepticus-induced memory deficits and dendritic damage. *PLoS One, 8*(3), e57808. doi: 10.1371/journal.pone.0057808

Buckmaster, P. S., & Lew, F. H. (2011). Rapamycin suppresses mossy fiber sprouting but not seizure frequency in a mouse model of temporal lobe epilepsy. *Journal of Neuroscience, 31*(6), 2337-2347.

Bye, N., Habgood, M. D., Callaway, J. K., Malakooti, N., Potter, A., Kossmann, T., & Morganti-Kossmann, M. C. (2007). Transient neuroprotection by minocycline following traumatic brain injury is associated with attenuated microglial activation but no changes in cell apoptosis or neutrophil infiltration. *Experimental Neurology, 204*(1), 220-233. doi: http://dx.doi.org/10.1016/j.expneurol.2006.10.013

Cavalheiro, E. A., Leite, J. P., Bortolotto, Z. A., Turski, W. A., Ikonomidou, C., & Turski, L. (1991). Long-Term Effects of Pilocarpine in Rats: Structural Damage of the Brain Triggers Kindling and Spontaneous I Recurrent Seizures. *Epilepsia, 32*(6), 778-782. doi: 10.1111/j.1528-1157.1991.tb05533.x

Chapman, M. G., Smith, M., & Hirsch, N. P. (2001). Status epilepticus. *Anaesthesia, 56*(7), 648-659. doi: 10.1046/j.1365-2044.2001.02115.x

Chauviere, L., Rafrafi, N., Thinus-Blanc, C., Bartolomei, F., Esclapez, M., & Bernard, C. (2009). Early deficits in spatial memory and theta rhythm in experimental temporal lobe epilepsy. *Journal of Neuroscience, 29*(17), 5402-5410. doi: 29/17/5402 [pii]

Chin, J., & Scharfman, H. E. (2013). Shared cognitive and behavioral impairments in epilepsy and Alzheimer's disease and potential underlying mechanisms. *Epilepsy & Behavior, 26*(3), 343-351. doi: 10.1016/j.yebeh.2012.11.040

Choi, J., & Koh, S. (2008). Role of brain inflammation in epileptogenesis. *Yonsei Medical Journal, 49*(1), 1-18. doi: 200802001 [pii]

Cowell, R. M., Plane, J. M., & Silverstein, F. S. (2003). Complement activation contributes to hypoxic-ischemic brain injury in neonatal rats. *The Journal of Neuroscience, 23*(28), 9459-9468.

Curia, G., Longo, D., Biagini, G., Jones, R. S., & Avoli, M. (2008). The pilocarpine model of temporal lobe epilepsy. *Journal of Neuroscience Methods, 172*(2), 143-157. doi: S0165-0270(08)00255-0 [pii]

Dachet, F., Bagla, S., Keren-Aviram, G., Morton, A., Balan, K., Saadat, L., . . . Loeb, J. A. (2015). Predicting novel histopathological microlesions in human epileptic brain through transcriptional clustering. *Brain, 138*(2), 356-370. doi: 10.1093/brain/awu350

De Simoni, M. G., Perego, C., Ravizza, T., Moneta, D., Conti, M., Marchesi, F., . . . Vezzani, A. (2000). Inflammatory cytokines and related genes are induced in the rat hippocampus by limbic status epilepticus. *European Journal of Neuroscience, 12*(7), 2623-2633. doi: ejn140 [pii]

De Simoni, M. G., Rossi, E., Storini, C., Pizzimenti, S., Echart, C., & Bergamaschini, L. (2004). The powerful neuroprotective action of C1-inhibitor on brain ischemia-reperfusion injury does not require C1q. *The American Journal of Pathology, 164*(5), 1857-1863. doi: http://dx.doi.org/10.1016/S0002-9440(10)63744-3

De Simoni, M. G., Storini, C., Barba, M., Catapano, L., Arabia, A. M., Rossi, E., & Bergamaschini, L. (2003). Neuroprotection by complement (C1) inhibitor in mouse transient brain ischemia. *Journal of Cerebral Blood Flow Metabolism, 23*(2), 232-239.

Dehmelt, L., & Halpain, S. (2004). The MAP2/Tau family of microtubule-associated proteins. *Genome Biology, 6*(1), 1-10. doi: 10.1186/gb-2004-6-1-204

Dingledine, R., Varvel, N., & Dudek, F. E. (2014). When and how do seizures kill neurons, and is cell death relevant to epileptogenesis? In H. E. Scharfman & P. S. Buckmaster (Eds.), *Issues in clinical epileptology: A view from the bench* (Vol. 813, pp. 109-122). Rotterdam, The Netherlands: Springer.

do Nascimento, A. L., Dos Santos, N. F., Campos Pelagio, F., Aparecida Teixeira, S., de Moraes Ferrari, E. A., & Langone, F. (2012). Neuronal degeneration and gliosis time-course in the mouse hippocampal formation after pilocarpine-induced status epilepticus. *Brain Research, 1470*, 98-110. doi: 10.1016/j.brainres.2012.06.008

Emmens, R. W., Naaijkens, B. A., Roem, D., Kramer, K., Wouters, D., Zeerleder, S., . . . Krijnen, P. A. (2013). Evaluating the efficacy of subcutaneous C1-esterase inhibitor administration for use in rat models of inflammatory diseases. *Drug Delivery*. doi: 10.3109/10717544.2013.853211

Eyo, U. B., Murugan, M., & Wu, L.-J. (2016). Microglia–neuron communication in epilepsy. *Glia*, n/a-n/a. doi: 10.1002/glia.23006

Eyo, U. B., Peng, J., Swiatkowski, P., Mukherjee, A., Bispo, A., & Wu, L.-J. (2014). Neuronal hyperactivity recruits microglial processes via neuronal NMDA receptors and microglial P2Y12 receptors after status epilepticus. *The Journal of Neuroscience, 34*(32), 10528-10540. doi: 10.1523/jneurosci.0416-14.2014

Eyupoglu, I. Y., Bechmann, I., & Nitsch, R. (2003). Modification of microglia function protects from lesion-induced neuronal alterations and promotes sprouting in the hippocampus. *FASEB Journal, 17*(9), 1110-1111. doi: 10.1096/fj.02-0825fje

Gardiner, J., Overall, R., & Marc, J. (2011). The microtubule cytoskeleton acts as a key downstream effector of neurotransmitter signaling. *Synapse, 65*(3), 249-256. doi: 10.1002/syn.20841

Gong, R., & Tang, S. J. (2006). Mitogen-activated protein kinase signaling is essential for activity-dependent dendritic protein synthesis. *Neuroreport, 17*(15), 1575-1578. doi: 10.1097/01.wnr.0000234742.42818.ff

Guerreiro, C. A. M., Jones-Gotman, M., Andermann, F., Bastos, A., & Cendes, F. (2001). Severe amnesia in epilepsy: Causes, anatomopsychological considerations, and treatment. *Epilepsy & Behavior, 2*(3), 224-246. doi: http://dx.doi.org/10.1006/ebeh.2001.0167

Guo, D., Zeng, L., Zou, J., Chen, L., Rensing, N., & Wong, M. (2016). Rapamycin prevents acute dendritic injury following seizures. *Annals of Clinical and Translational Neurology, 3*(3), 180-190. doi: 10.1002/acn3.284

Harada, A., Teng, J., Takei, Y., Oguchi, K., & Hirokawa, N. (2002). MAP2 is required for dendrite elongation, PKA anchoring in dendrites, and proper PKA signal transduction. *Journal of Cellular Biology, 158*(3), 541-549. doi: 10.1083/jcb.200110134

Hasegawa, S., Yamaguchi, M., Nagao, H., Mishina, M., & Mori, K. (2007). Enhanced cell-to-cell contacts between activated microglia and pyramidal cell dendrites following kainic acid-induced neurotoxicity in the hippocampus. *Journal of Neuroimmunology, 186*(1-2), 75-85. doi: 10.1016/j.jneuroim.2007.03.005

Heydenreich, N., Nolte, M. W., Gob, E., Langhauser, F., Hofmeister, M., Kraft, P., . . . Kleinschnitz, C. (2012). C1-inhibitor protects from brain ischemia-reperfusion injury by combined antiinflammatory and antithrombotic mechanisms. *Stroke, 43*(9), 2457-2467. doi: 10.1161/STROKEAHA.112.660340

Holmes, G. L. (2004). Effects of early seizures on later behavior and epileptogenicity. *Mental Retardation and Dev Disabilities Research Reviews, 10*(2), 101-105. doi: 10.1002/mrdd.20019

Hong, S., Beja-Glasser, V. F., Nfonoyim, B. M., Frouin, A., Li, S., Ramakrishnan, S., . . . Stevens, B. (2016). Complement and microglia mediate early synapse loss in Alzheimer mouse models. *Science*. doi: 10.1126/science.aad8373

Horn, K. P., Busch, S. A., Hawthorne, A. L., van Rooijen, N., & Silver, J. (2008). Another barrier to regeneration in the CNS: Activated macrophages induce extensive retraction of dystrophic axons through direct physical interactions. *Journal of Neuroscience, 28*(38), 9330-9341. doi: 28/38/9330 [pii]

Hort, J., Brożek, G., Mareš, P., Langmeier, M., & Komárek, V. (1999). Cognitive functions after pilocarpine-induced status epilepticus: changes during silent period precede appearance of spontaneous recurrent seizures. *Epilepsia, 40*(9), 1177-1183. doi: 10.1111/j.1528-1157.1999.tb00845.x

Huang, X., Zhang, H., Yang, J., Wu, J., McMahon, J., Lin, Y., . . . Huang, Y. (2010). Pharmacological inhibition of the mammalian target of rapamycin pathway suppresses acquired epilepsy. *Neurobiology Disease, 40*(1), 193-199. doi: S0969-9961(10)00186-5 [pii]

Jacobs, M. P., Leblanc, G. G., Brooks-Kayal, A., Jensen, F. E., Lowenstein, D. H., Noebels, J. L., . . . Swann, J. W. (2009). Curing epilepsy: Progress and future directions. *Epilepsy and Behavior, 14*(3), 438-445. doi: S1525-5050(09)00097-3 [pii]

Jalava, N. S., Lopez-Picon, F. R., Kukko-Lukjanov, T. K., & Holopainen, I. E. (2007). Changes in microtubule-associated protein-2 (MAP2) expression during development and after status epilepticus in the immature rat hippocampus. *International Journal of Developmental Neuroscience, 25*(2), 121-131. doi: S0736-5748(06)00452-7 [pii]

Jefferys, J. G. R. (2010). Advances in understanding basic mechanisms of epilepsy and seizures. *Seizure, 19*(10), 638-646. doi: http://dx.doi.org/10.1016/j.seizure.2010.10.026

Jung, K.-H., Chu, K., Lee, S.-T., Kim, J.-H., Kang, K.-M., Song, E.-C., . . . Roh, J.-K. (2009). Region-specific plasticity in the epileptic rat brain: A hippocampal and extrahippocampal analysis. *Epilepsia, 50*(3), 537-549. doi: 10.1111/j.1528-1167.2008.01718.x

Kettenmann, H., Hanisch, U. K., Noda, M., & Verkhratsky, A. (2011). Physiology of microglia. *Physiological Reviews, 91*(2), 461-553. doi: 10.1152/physrev.00011.2010

Kettenmann, H., Kirchhoff, F., & Verkhratsky, A. (2013). Microglia: New roles for the synaptic stripper. *Neuron, 77*(1), 10-18. doi: http://dx.doi.org/10.1016/j.neuron.2012.12.023

Kolev, M. V., Ruseva, M. M., Harris, C. L., Morgan, B. P., & Donev, R. M. (2009). Implication of complement system and its regulators in Alzheimer's disease. *Current Neuropharmacology, 7*(1), 1-8. doi: 10.2174/157015909787602805

Leite, J. P., Bortolotto, Z. A., & Cavalheiro, E. A. (1990). Spontaneous recurrent seizures in rats: An experimental model of partial epilepsy. *Neuroscience & Biobehavioral Reviews, 14*(4), 511-517. doi: http://dx.doi.org/10.1016/S0149-7634(05)80076-4

Lesting, J., Geiger, M., Narayanan, R. T., Pape, H. C., & Seidenbecher, T. (2011). Impaired extinction of fear and maintained amygdala-hippocampal theta synchrony in a mouse model of temporal lobe epilepsy. *Epilepsia, 52*(2), 337-346. doi: 10.1111/j.1528-1167.2010.02758.x

Levin, J. R., Serrano, G., & Dingledine, R. (2012). Reduction in delayed mortality and subtle improvement in retrograde memory performance in pilocarpine-treated mice with conditional neuronal deletion of cyclooxygenase-2 gene. *Epilepsia, 53*(8), 1411-1420. doi: 10.1111/j.1528-1167.2012.03584.x

Libbey, J. E., Kirkman, N. J., Wilcox, K. S., White, H. S., & Fujinami, R. S. (2010). Role for complement in the development of seizures following acute viral infection. *Journal of Virology, 84*(13), 6452-6460. doi: 10.1128/JVI.00422-10

Locklear, M. N., & Kritzer, M. F. (2014). Assessment of the effects of sex and sex hormones on spatial cognition in adult rats using the Barnes maze. *Hormones and Behavior, 66*(2), 298-308. doi: http://dx.doi.org/10.1016/j.yhbeh.2014.06.006

Lugo, J. N., Barnwell, L. F., Ren, Y., Lee, W. L., Johnston, L. D., Kim, R., . . . Anderson, A. E. (2008). Altered phosphorylation and localization of the A-type channel, Kv4.2 in status epilepticus. *Journal of Neurochemistry, 106*(4), 1929-1940. doi: JNC5508 [pii]

Ma, Y., Ramachandran, A., Ford, N., Parada, I., & Prince, D. A. (2013). Remodeling of dendrites and spines in the C1q knockout model of genetic epilepsy. *Epilepsia, 54*(7), 1232-1239. doi: 10.1111/epi.12195

Martinez-Saguer, I., Cicardi, M., Suffritti, C., Rusicke, E., Aygören-Pürsün, E., Stoll, H., . . . Kreuz, W. (2014). Pharmacokinetics of plasma-derived C1-esterase inhibitor after subcutaneous versus intravenous administration in subjects with mild or moderate hereditary angioedema: The PASSION study. *Transfusion, 54*(6), 1552-1561. doi: 10.1111/trf.12501

Michailidou, I., Willems, J. G. P., Kooi, E.-J., van Eden, C., Gold, S. M., Geurts, J. J. G., . . . Ramaglia, V. (2015). Complement C1q-C3–associated synaptic changes in multiple sclerosis hippocampus. *Annals of Neurology, 77*(6), 1007-1026. doi: 10.1002/ana.24398

Mirrione, M. M., & Tsirka, S. E. (2011). A functional role for microglia in epilepsy. *Clinical and Genetic Aspects of Epilepsy*.

Moser, M.-B., & Moser, E. I. (1998). Functional differentiation in the hippocampus. *Hippocampus, 8*(6), 608-619. doi: 10.1002/(SICI)1098-1063(1998)8:6<608::AID-HIPO3>3.0.CO;2-7

Muller, C. J., Bankstahl, M., Groticke, I., & Loscher, W. (2009). Pilocarpine vs. lithium-pilocarpine for induction of status epilepticus in mice: development of spontaneous seizures, behavioral alterations and neuronal damage. *European Journal of Pharmacology, 619*(1-3), 15-24. doi: S0014-2999(09)00612-8 [pii]

Murphy, G. G. (2013). Spatial learning and memory—What's TLE got to do with it? *Epilepsy Currents, 13*(1), 26-29. doi: 10.5698/1535-7511-13.1.26

Nair, P. P., Kalita, J., & Misra, U. K. (2011). Status epilepticus: Why, what, and how. *Journal of Postgraduate Medicine, 57*(3), 242-252.

Neppe, V. (1981). Symptomatology of temporal lobe epilepsy. *South Africian Medical Journal, 60*(23), 902-907.

Nielsen, E. W., Waage, C., Fure, H., Brekke, O. L., Sfyroera, G., Lambris, J. D., & Mollnes, T. E. (2007). Effect of supraphysiologic levels of C1-inhibitor on the classical, lectin and alternative pathways of complement. *Molecular Immunology, 44*(8), 1819-1826. doi: 10.1016/j.molimm.2006.10.003

Nimmerjahn, A., Kirchhoff, F., & Helmchen, F. (2005). Resting microglial cells are highly dynamic surveillants of brain parenchyma in vivo. *Science, 308*(5726), 1314-1318. doi: 10.1126/science.1110647

Nolan, M. A., Redoblado, M. A., Lah, S., Sabaz, M., Lawson, J. A., Cunningham, A. M., . . . Bye, A. M. (2003). Intelligence in childhood epilepsy syndromes. *Epilepsy Research, 53*(1-2), 139-150. doi: S0920121102002619 [pii]

Paolicelli, R. C., Bolasco, G., Pagani, F., Maggi, L., Scianni, M., Panzanelli, P., . . . Gross, C. T. (2011). Synaptic pruning by microglia is necessary for normal brain development. *Science, 333*(6048), 1456-1458. doi: science.1202529 [pii]

Patterson, K. P., Brennan, G. P., Curran, M., Kinney-Lang, E., Dube, C., Rashid, F., . . . Baram, T. Z. (2015). Rapid, coordinate inflammatory responses after experimental febrile status epilepticus: Implications for epileptogenesis. *eNeuro, 2*(5), e0034-0015.2015. doi: 10.1523/ENEURO.0034-15.2015

Pearson, J. N., Schulz, K. M., & Patel, M. (2014). Specific alterations in the performance of learning and memory tasks in models of chemoconvulsant-induced status epilepticus. *Epilepsy Reseach, 108*(6), 1032-1040.

Perez-Alcazar, M., Daborg, J., Stokowska, A., Wasling, P., Björefeldt, A., Kalm, M., . . . Pekna, M. (2014). Altered cognitive performance and synaptic function in the hippocampus of mice lacking C3. *Experimental Neurology, 253*, 154-164. doi: http://dx.doi.org/10.1016/j.expneurol.2013.12.013

Racine, R. J. (1972). Modification of seizure activity by electrical stimulation. II. Motor seizure. *Electroencephalography and Clinical Neurophysiology, 32*(3), 281-294.

Ramos, F. O., Carreiro, L. R. R., Scorza, F. A., & Cysneiros, R. M. (2016). Impaired executive functions in experimental model of temporal lobe epilepsy. *Arquivos de Neuro-Psiquiatria, 74*, 470-477.

Rao, M. S., Hattiangady, B., Reddy, D. S., & Shetty, A. K. (2006). Hippocampal neurodegeneration, spontaneous seizures, and mossy fiber sprouting in the F344 rat model of temporal lobe epilepsy. *Journal of Neuroscience Research, 83*(6), 1088-1105. doi: 10.1002/jnr.20802

Ravizza, T., Rizzi, M., Perego, C., Richichi, C., Veliskova, J., Moshe, S. L., . . . Vezzani, A. (2005). Inflammatory response and glia activation in developing rat hippocampus after status epilepticus. *Epilepsia, 46* (5), 113-117. doi: EPI01006 [pii]

Richwine, A. F., Parkin, A. O., Buchanan, J. B., Chen, J., Markham, J. A., Juraska, J. M., & Johnson, R. W. (2008). Architectural changes to CA1 pyramidal neurons in adult and aged mice after peripheral immune stimulation. *Psychoneuroendocrinology, 33*(10), 1369-1377. doi: 10.1016/j.psyneuen.2008.08.003

Rizzi, M., Perego, C., Aliprandi, M., Richichi, C., Ravizza, T., Colella, D., . . . Vezzani, A. (2003). Glia activation and cytokine increase in rat hippocampus by kainic acid-induced status epilepticus during postnatal development. *Neurobiology Disease, 14*(3), 494-503. doi: S0969996103001499 [pii]

Sanchez, C., Diaz-Nido, J., & Avila, J. (2000). Phosphorylation of microtubule-associated protein 2 (MAP2) and its relevance for the regulation of the neuronal cytoskeleton function. *Progress in Neurobiology, 61*(2), 133-168.

Sarma, J. V., & Ward, P. A. (2011). The complement system. *Cell and Tissue Research, 343*(1), 227-235. doi: 10.1007/s00441-010-1034-0

Schafer, D. P., Lehrman, E. K., Kautzman, A. G., Koyama, R., Mardinly, A. R., Yamasaki, R., . . . Stevens, B. (2012). Microglia sculpt postnatal neural circuits in an activity and complement-dependent manner. *Neuron, 74*(4), 691-705. doi: 10.1016/j.neuron.2012.03.026

Schafer, D. P., Lehrman, E. K., & Stevens, B. (2013). The "quad-partite" synapse: Microglia-synapse interactions in the developing and mature CNS. *Glia, 61*(1), 24-36. doi: 10.1002/glia.22389

Scharfman, H. E. (2007). The neurobiology of epilepsy. *Current Neurology and Neuroscience Reports, 7*(4), 348-354.

Scharfman, H. E. (2014). Epilepsy. In M. J. Zigmond, J. T. Coyle & L. P. Rowland (Eds.), *Neurobiology of brain disorders: Biological basis of neurological and psychiatric disorders* (pp. 236-261). London, United Kingdom: Elsevier.

Schartz, N. D., Herr, S. A., Madsen, L., Butts, S. J., Torres, C., Mendez, L. B., & Brewster, A. L. (2016). Spatiotemporal profile of Map2 and microglial changes in the hippocampal CA1 region following pilocarpine-induced status epilepticus. *Scientific Reports, 6*, 24988. doi: 10.1038/srep24988 http://www.nature.com/articles/srep24988#supplementary-information

Schenk, F., & Morris, R. (1985). Dissociation between components of spatial memory in rats after recovery from the effects of retrohippocampal lesions. *Experimental Brain Research, 58*(1), 11-28.

Scoville, W. B., & Milner, B. (1957). Loss of recent memory after bilateral hippocampal lesions. *Journal of Neurology, Neurosurgery, and Psychiatry, 20*(1), 11-21.

Shapiro, L. A., Korn, M. J., & Ribak, C. E. (2005). Newly generated dentate granule cells from epileptic rats exhibit elongated hilar basal dendrites that align along GFAP-immunolabeled processes. *Neuroscience, 136*(3), 823-831. doi: S0306-4522(05)00448-3 [pii]

Shapiro, L. A., Wang, L., & Ribak, C. E. (2008). Rapid astrocyte and microglial activation following pilocarpine-induced seizures in rats. *Epilepsia, 49*(2), 33-41. doi: EPI1491 [pii]

Sierra, A., Abiega, O., Shahraz, A., & Neumann, H. (2013). Janus-faced microglia: beneficial and detrimental consequences of microglial phagocytosis. *Frontiers in Cellular Neuroscience, 7*, 6. doi: 10.3389/fncel.2013.00006

Silverman, S. M., Kim, B.-J., Howell, G. R., Miller, J., John, S. W. M., Wordinger, R. J., & Clark, A. F. (2016). C1q propagates microglial activation and neurodegeneration in the visual axis following retinal ischemia/reperfusion injury. *Molecular Neurodegeneration, 11*(1), 1-16. doi: 10.1186/s13024-016-0089-0

Stafstrom, C. E. (2014). Epilepsy comorbidities: How can animal models help? *Advances in Experimental Medicine and Biology, 813*, 273-281. doi: 10.1007/978-94-017-8914-1_22

Steinlein, O. K. (2004). Genetic mechanisms that underlie epilepsy. *Nature, 5*, 400-408. doi: doi:10.1038/nrn1388

Stephan, A. H., Barres, B. A., & Stevens, B. (2012). The complement system: an unexpected role in synaptic pruning during development and disease. *Annual Review of Neuroscience, 35*, 369-389. doi: 10.1146/annurev-neuro-061010-113810

Stevens, B., Allen, N. J., Vazquez, L. E., Howell, G. R., Christopherson, K. S., Nouri, N., . . . Barres, B. A. (2007). The classical complement cascade mediates CNS synapse elimination. *Cell, 131*(6), 1164-1178. doi: 10.1016/j.cell.2007.10.036

Swann, J. W., Al-Noori, S., Jiang, M., & Lee, C. L. (2000). Spine loss and other dendritic abnormalities in epilepsy. *Hippocampus, 10*(5), 617-625. doi: 10.1002/1098-1063(2000)10:5<617::AID-HIPO13>3.0.CO;2-R

Swann, J. W., & Hablitz, J. J. (2000). Cellular abnormalities and synaptic plasticity in seizure disorders of the immature nervous system. *Mental Retardation and Developmental Disabilities Research Reviews, 6*(4), 258-267. doi: 10.1002/1098-2779(2000)6:4<258::AID-MRDD5>3.0.CO;2-H [pii]

Swann, J. W., & Rho, J. M. (2014). How is homeostatic plasticity important in epilepsy? *Advances in Experimental Medicine and Biology, 813*, 123-131. doi: 10.1007/978-94-017-8914-1_10

Szyndler, J., Wierzba-Bobrowicz, T., Skorzewska, A., Maciejak, P., Walkowiak, J., Lechowicz, W., . . . Plaznik, A. (2005). Behavioral, biochemical and histological studies in a model of pilocarpine-induced spontaneous recurrent seizures. *Pharmacology Biochemistry and Behavior, 81*(1), 15-23. doi: 10.1016/j.pbb.2005.01.020

Téllez-Zenteno, J. F., & Hernández-Ronquillo, L. (2012). A review of the epidemiology of temporal lobe epilepsy. *Epilepsy Research and Treatment, 2012*, 5. doi: 10.1155/2012/630853

Thurman, D. J., Beghi, E., Begley, C. E., Berg, A. T., Buchhalter, J. R., Ding, D., . . . for the, I. C. o. E. (2011). Standards for epidemiologic studies and surveillance of epilepsy. *Epilepsia, 52*, 2-26. doi: 10.1111/j.1528-1167.2011.03121.x

Tremblay, M. E., Stevens, B., Sierra, A., Wake, H., Bessis, A., & Nimmerjahn, A. (2011). The role of microglia in the healthy brain. *Journal of Neuroscience, 31*(45), 16064-16069. doi: 10.1523/JNEUROSCI.4158-11.2011

Turrin, N. P., & Rivest, S. (2004). Innate immune reaction in response to seizures: Implications for the neuropathology associated with epilepsy. *Neurobiology of Disease, 16*(2), 321-334. doi: http://dx.doi.org/10.1016/j.nbd.2004.03.010

Urbanska, M., Blazejczyk, M., & Jaworski, J. (2008). Molecular basis of dendritic arborization. *Acta Neurobiologiae Experimentalis (Wars), 68*(2), 264-288.

Väkevä, A., Morgan, B. P., Tikkanen, I., Helin, K., Laurila, P., & Meri, S. (1994). Time course of complement activation and inhibitor expression after ischemic injury of rat myocardium. *The American Journal of Pathology, 144*(6), 1357-1368.

van Vliet, E. A., Forte, G., Holtman, L., den Burger, J. C., Sinjewel, A., de Vries, H. E., . . . Gorter, J. A. (2012). Inhibition of mammalian target of rapamycin reduces epileptogenesis and blood-brain barrier leakage but not microglia activation. *Epilepsia, 53*(7), 1254-1263. doi: 10.1111/j.1528-1167.2012.03513.x

Vezzani, A., Conti, M., De Luigi, A., Ravizza, T., Moneta, D., Marchesi, F., & De Simoni , M. G. (1999). Interleukin-1β immunoreactivity and microglia are enhanced in the rat hippocampus by focal kainate application: Functional evidence for enhancement of electrographic seizures. *The Journal of Neuroscience, 19*(12), 5054-5065.

Vezzani, A., French, J., Bartfai, T., & Baram, T. Z. (2011). The role of inflammation in epilepsy. *Nature Reviews Neurology, 7*(1), 31-40. doi: nrneurol.2010.178 [pii]

Vezzani, A., & Granata, T. (2005). Brain inflammation in epilepsy: Experimental and clinical evidence. *Epilepsia, 46*(11), 1724-1743. doi: EPI298 [pii]

Wang, N., Mi, X., Gao, B., Gu, J., Wang, W., Zhang, Y., & Wang, X. (2015). Minocycline inhibits brain inflammation and attenuates spontaneous recurrent seizures following pilocarpine-induced status epilepticus. *Neuroscience, 287*, 144-156. doi: http://dx.doi.org/10.1016/j.neuroscience.2014.12.021

Wiebe, S. (2000). Epidemiology of temporal lobe epilepsy. *Canadian Journal of Neurological Sciences / Journal Canadien des Sciences Neurologiques, 27*(SupplementS1), S6-S10. doi: doi:10.1017/S0317167100000561

Wong, M. (2005). Modulation of dendritic spines in epilepsy: Cellular mechanisms and functional implications. *Epilepsy and Behavior, 7*(4), 569-577. doi: S1525-5050(05)00317-3 [pii]

Wong, M., & Guo, D. (2013). Dendritic spine pathology in epilepsy: Cause or consequence? *Neuroscience, 251*, 141-150. doi: 10.1016/j.neuroscience.2012.03.048

Yang, F., Liu, Z. R., Chen, J., Zhang, S. J., Quan, Q. Y., Huang, Y. G., & Jiang, W. (2010). Roles of astrocytes and microglia in seizure-induced aberrant neurogenesis in the hippocampus of adult rats. *Journal of Neuroscience Research, 88*(3), 519-529. doi: 10.1002/jnr.22224

Zeng, L. H., Rensing, N. R., & Wong, M. (2009). The mammalian target of rapamycin signaling pathway mediates epileptogenesis in a model of temporal lobe epilepsy. *Journal of Neurosci, 29*(21), 6964-6972. doi: 29/21/6964 [pii]